

Supplementary Information for

Iridium Porphyrin Complexes with μ -Nitrido, Hydroxo, Hydrosulfido and
Alkynyl Ligands

Shiu-Chun So, Wai-Man Cheung*, Wai-Hang Chiu, Matthew de Vere-Tucker, Herman H. Y. Sung, Ian D. Williams*, and Wa-Hung Leung*

*Department of Chemistry, The Hong Kong University of Science and Technology,
Clear Water Bay, Kowloon, Hong Kong, People's Republic of China*

*Corresponding authors, E-mail: cheungwm@ust.hk, chleung@ust.hk

Table of Content

	Page no.
1. Crystallographic data and experimental details for 3 , 4 , 7 , 8 , 9 and 10	2
2. NMR spectra	3-22
3. Preliminary molecular structure of $[\text{Ir}(\text{tpp})(\text{PPh}_3)(\text{H}_2\text{O})](\text{SbCl}_6)$	23
4. UV-vis spectra	24-27
5. Cyclic voltammograms	28-30

Table S1. Crystallographic data and experimental details for **3**, **4**, **7**, **8**, **9** and **10**.

	3 ·C ₆ H ₁₄	4 ·CH ₂ Cl ₂	7·0.5C ₄ H ₈ O·0.5H ₂ O	8 ·0.825C ₄ H ₁₀ O	9 ·0.75C ₄ H ₈ O	10
Formula	C ₇₅ H ₉₀ Cl ₂ CoIrN ₅ O ₉ P ₃ Ru	C ₆₂ H ₆₅ Cl ₅ CoIrN ₅ O ₉ P ₃ Ru	C ₁₂₈ H ₉₈ Ir ₂ N ₈ O ₄ P ₂	C _{73.3} H _{56.25} CuIIrN ₄ O _{0.82} P	C ₇₃ H ₅₄ IrN ₄ O _{0.75} P	C ₆₂ H ₄₄ IrN ₄ PS
Formula weight	1721.52	1646.55	2258.48	1419.88	1222.37	1100.24
Crystal system	Triclinic	monoclinic	orthorhombic	monoclinic	orthorhombic	triclinic
Space group	P-1	P2 ₁ /n	Pca2 ₁	Pc	Pbca	P-1
<i>a</i> , Å	13.0825(3)	13.4813(2)	26.2427(2)	50.7613(8)	19.8221(4)	10.0055(4)
<i>b</i> , Å	13.8500(5)	29.6101(6)	10.41332(13)	11.4855(2)	21.8692(4)	14.3928(6)
<i>c</i> , Å	20.4656(5)	16.4218(2)	35.1224(3)	20.6642(3)	25.5085(5)	17.7170(7)
α , deg	85.316(2)	90.00	90	90	90	97.827(3)
β , deg	80.0763(19)	101.0227(15)	90	90.0435(13)	90	98.001(3)
γ , deg	78.870(2)	90.00	90	90	90	107.838(4)
<i>V</i> , Å ³	3579.55(17)	6434.3(2)	9598.03(17)	12047.6(3)	11057.7(4)	2361.41(17)
<i>Z</i>	2	4	4	8	8	2
ρ_{calc} , g cm ⁻³	1.597	1.700	1.563	1.566	1.469	1.547
<i>T</i> , K	99.9(4)	99.9(5)	100.10(10)	100.15	100.01(10)	100.00(10)
μ , mm ⁻¹	8.818	10.901	6.115	3.148	2.495	6.568
<i>F</i> (000)	1748.0	3288.0	4552.0	5637.0	4944.0	1104.0
Total reflections	20356	28639	30575	66719	62021	13649
Independent reflections	12629	11287	14064	40951	10817	8385
<i>R</i> _{int}	0.0216	0.0441	0.0284	0.0419	0.1519	0.0269
GoF ^a	1.012	1.003	1.002	1.089	1.001	1.001
<i>R</i> ₁ , ^b <i>wR</i> ₂ ^c [<i>I</i> > 2σ(<i>I</i>)]	0.0291, 0.0763	0.0414, 0.1020	0.0267, 0.0655	0.0755, 0.1747	0.0514, 0.1033	0.0246,
<i>R</i> ₁ , <i>wR</i> ₂ (all data)	0.0312, 0.0777	0.0519, 0.1076	0.0282, 0.0665	0.0923, 0.1876	0.0931, 0.1186	0.0285,

^a GoF = [Σ*w*(|*F*_o| - |*F*_c|)²/(*N*_{obs} - *N*_{param})]^{1/2}. ^b *R*₁ = Σ|*F*_o| - |*F*_c|/Σ|*F*_o|. ^c *wR*₂ [(Σ*w*|*F*_o| - |*F*_c|)²/Σ*w*²|*F*_o|]

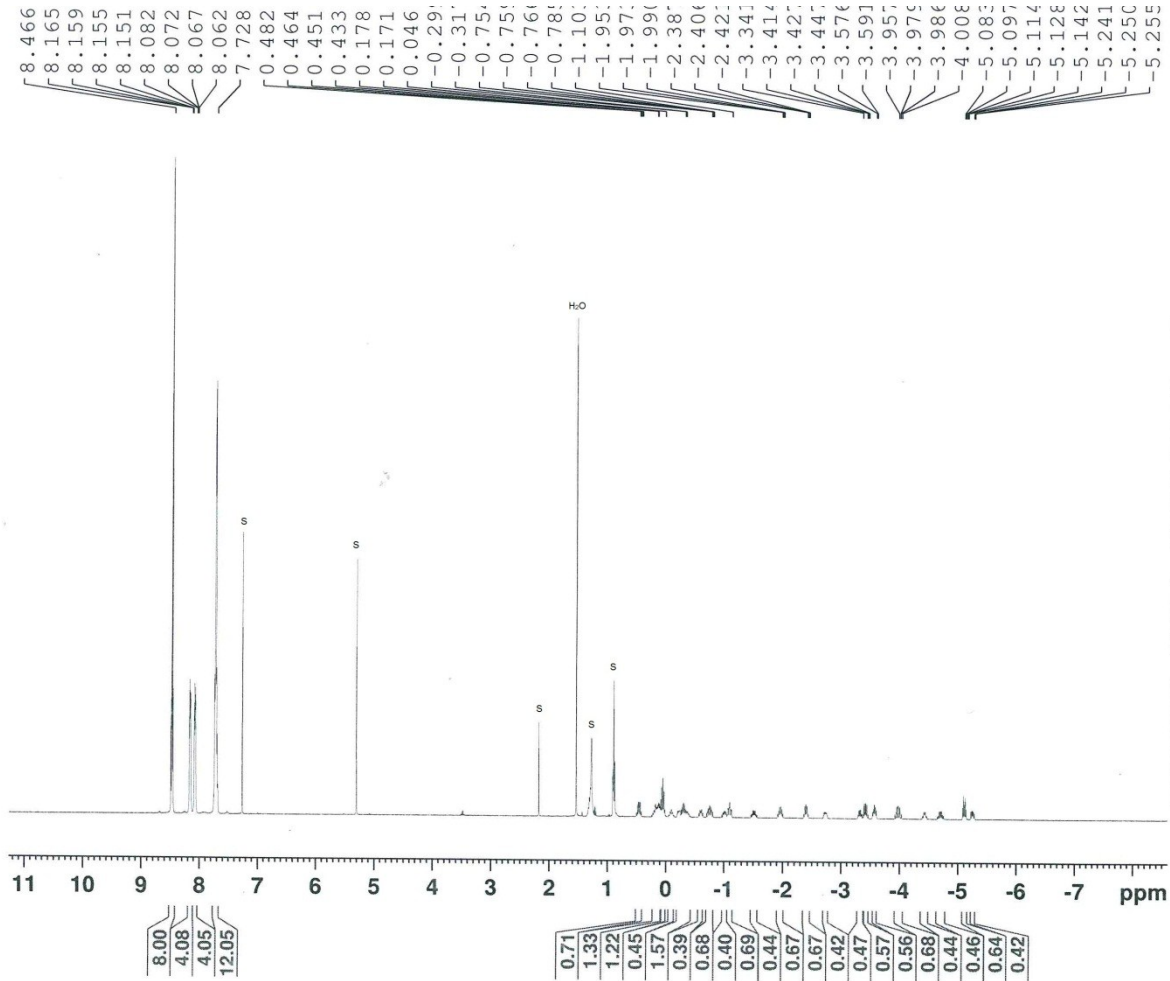


Figure S1. ^1H NMR (400 MHz, 298 K, CDCl_3) spectrum of **1** (X = impurity, S = residual solvent).

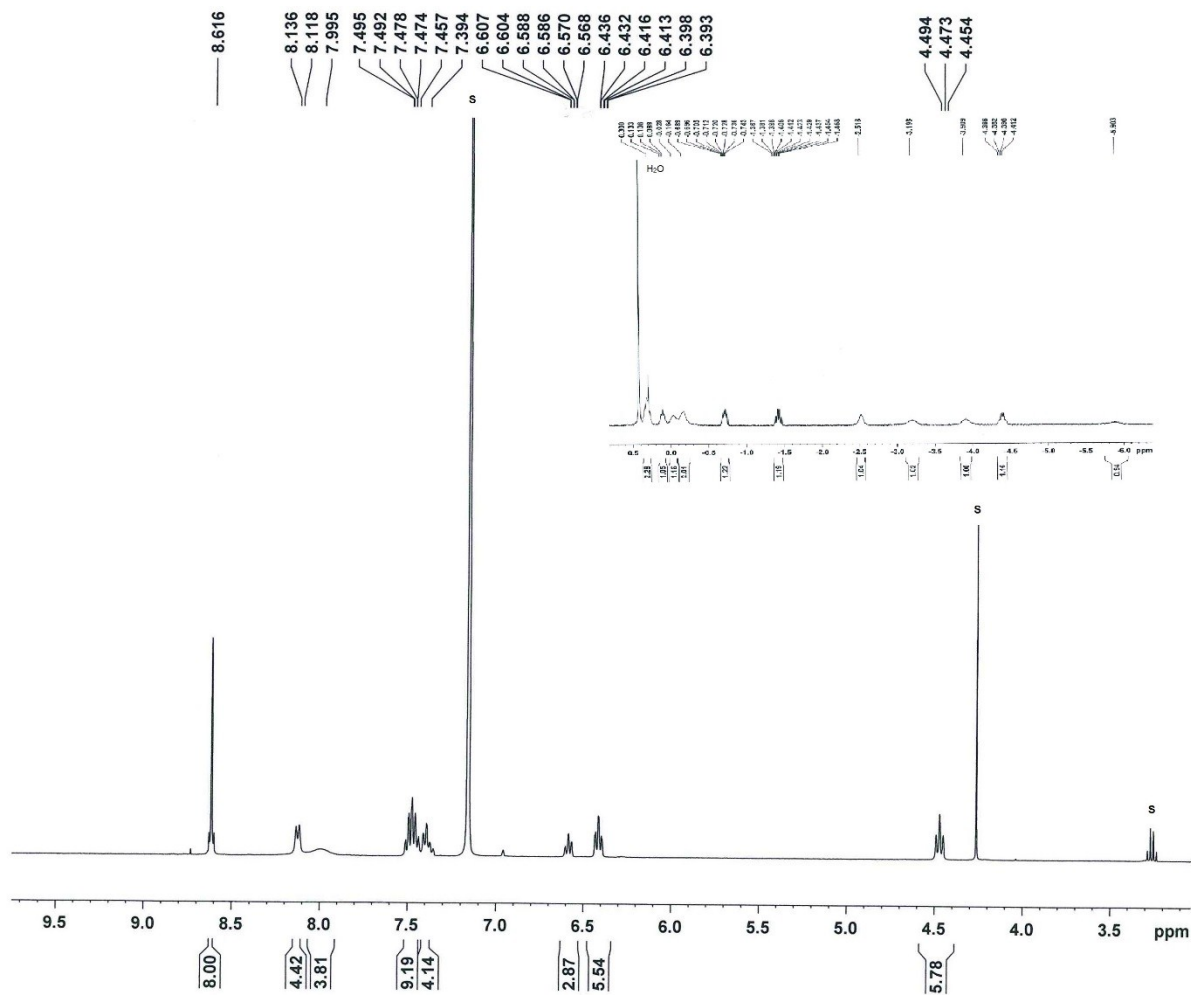


Figure S2. ^1H NMR (400 MHz, 298 K, C_6D_6) spectrum of **2** (X = impurity, S = residual solvent).

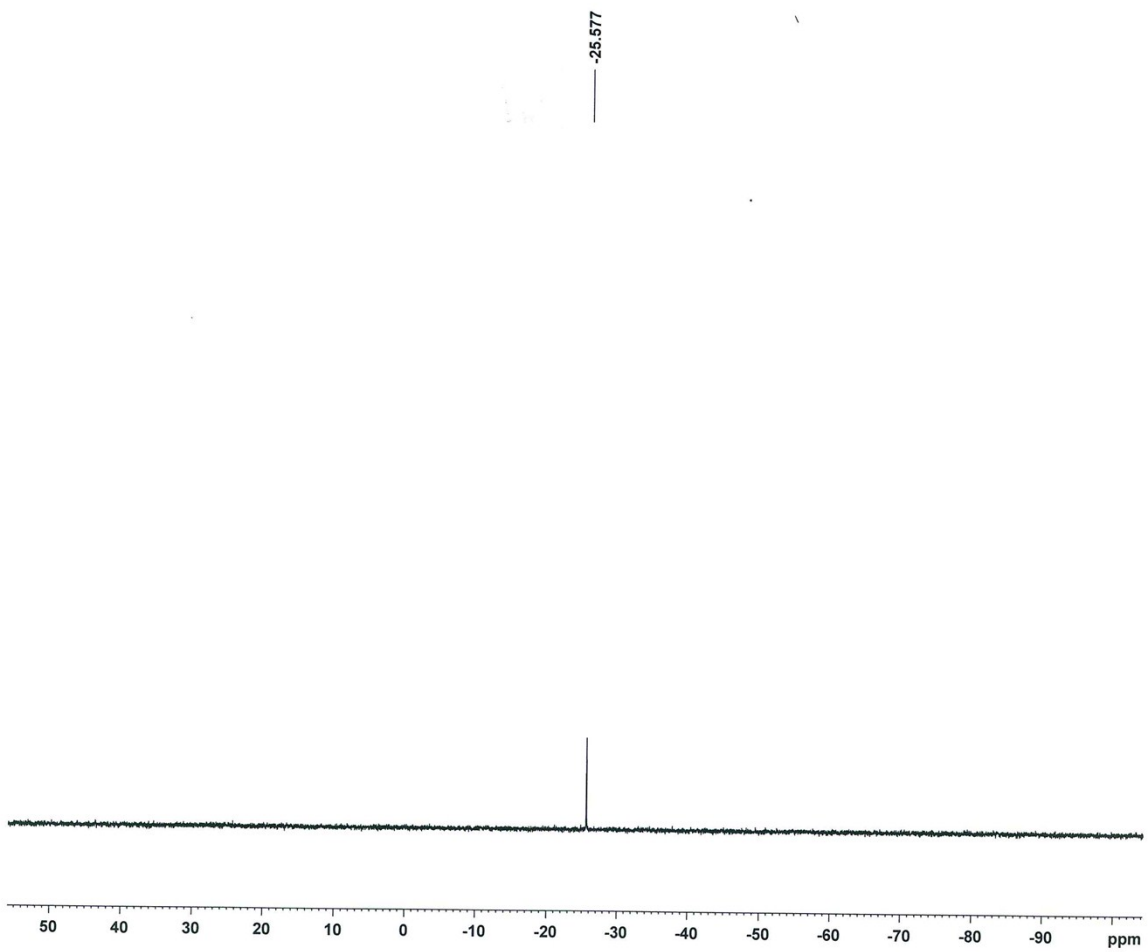


Figure S3. $^{31}\text{P}\{\text{H}\}$ NMR (162 MHz, 298 K, C_6D_6) spectrum of **2**.

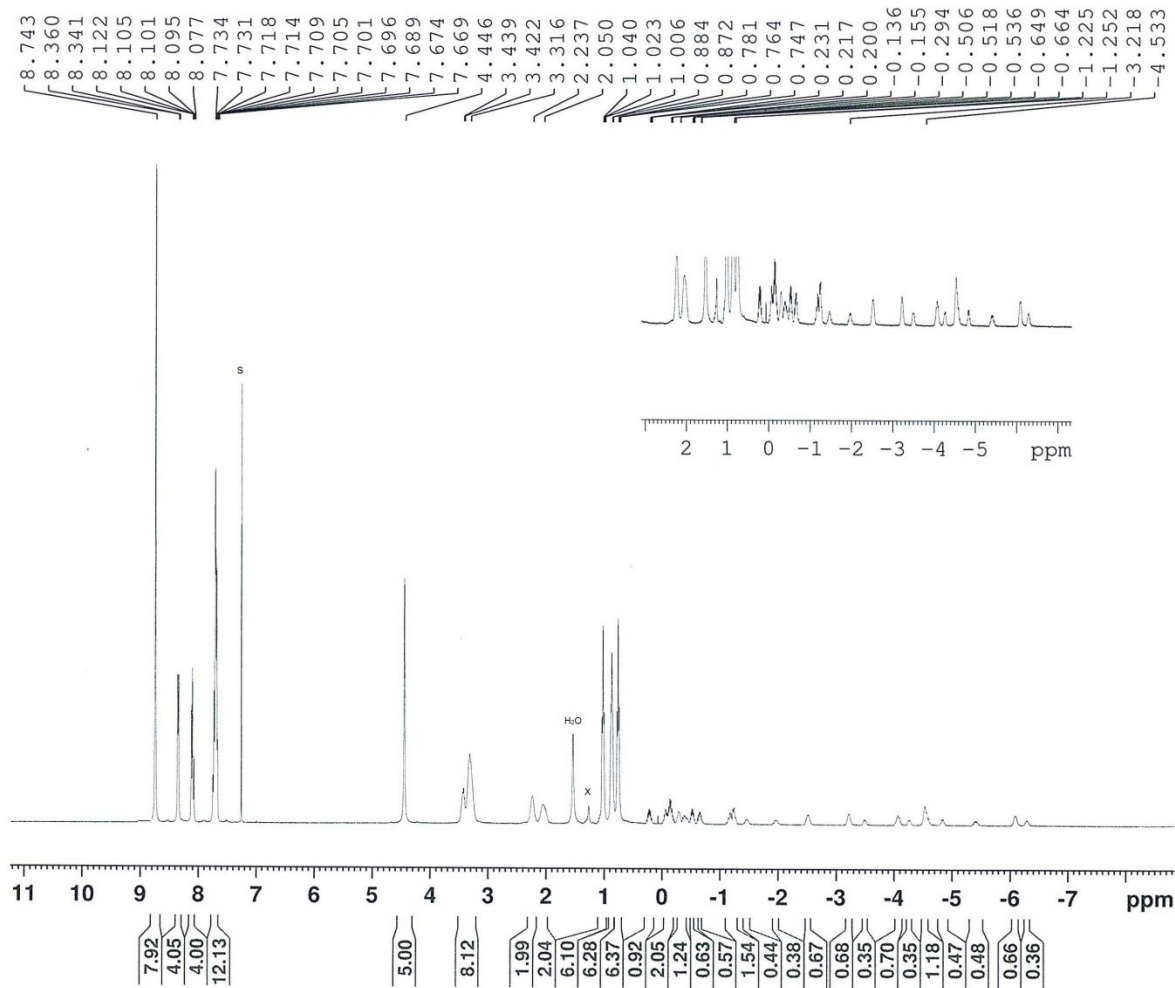


Figure S4. ^1H NMR (400 MHz, 298 K, CDCl_3) spectrum of **3** (X = impurity, S = residual solvent).

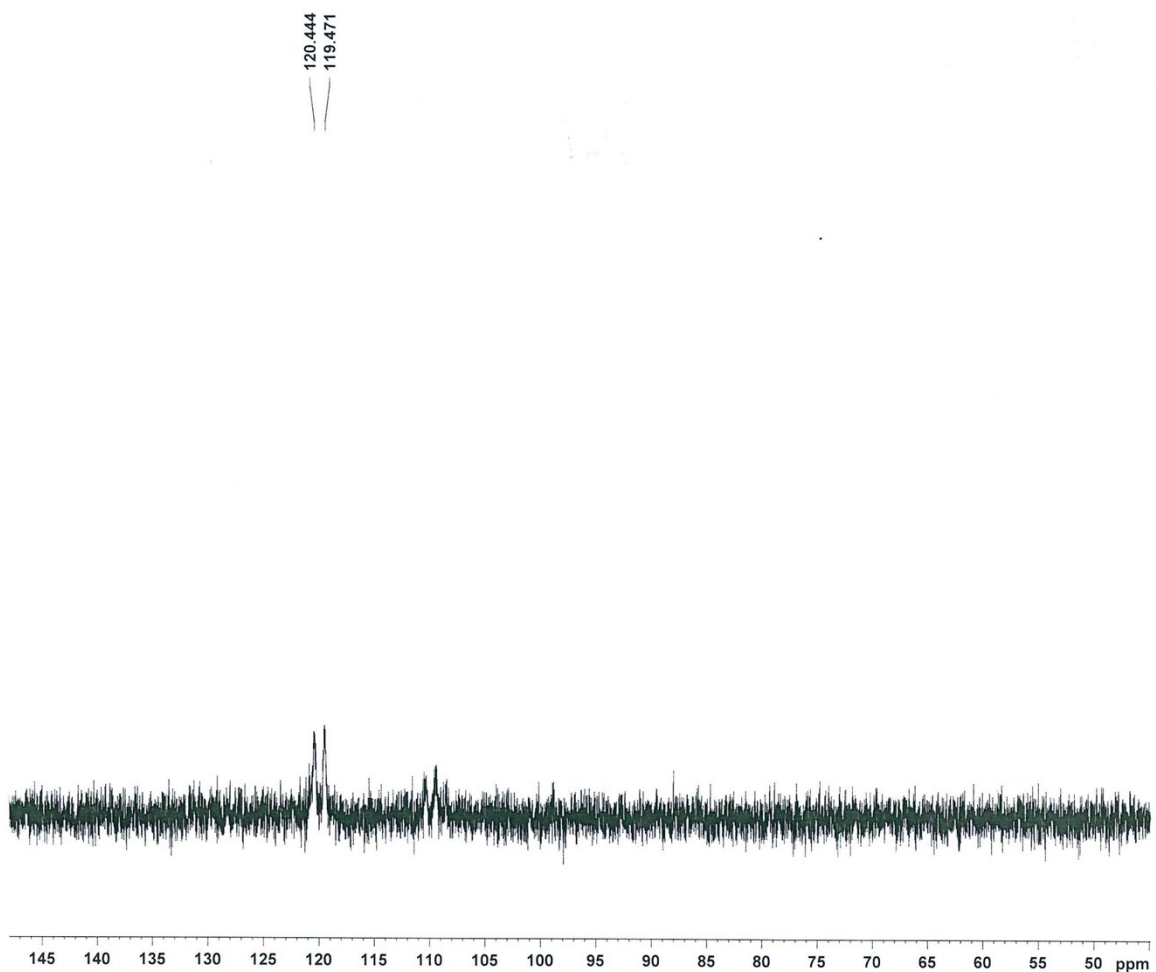


Figure S5. $^{31}\text{P}\{\text{H}\}$ NMR (162 MHz, 298 K, CDCl_3) spectrum of **3**.

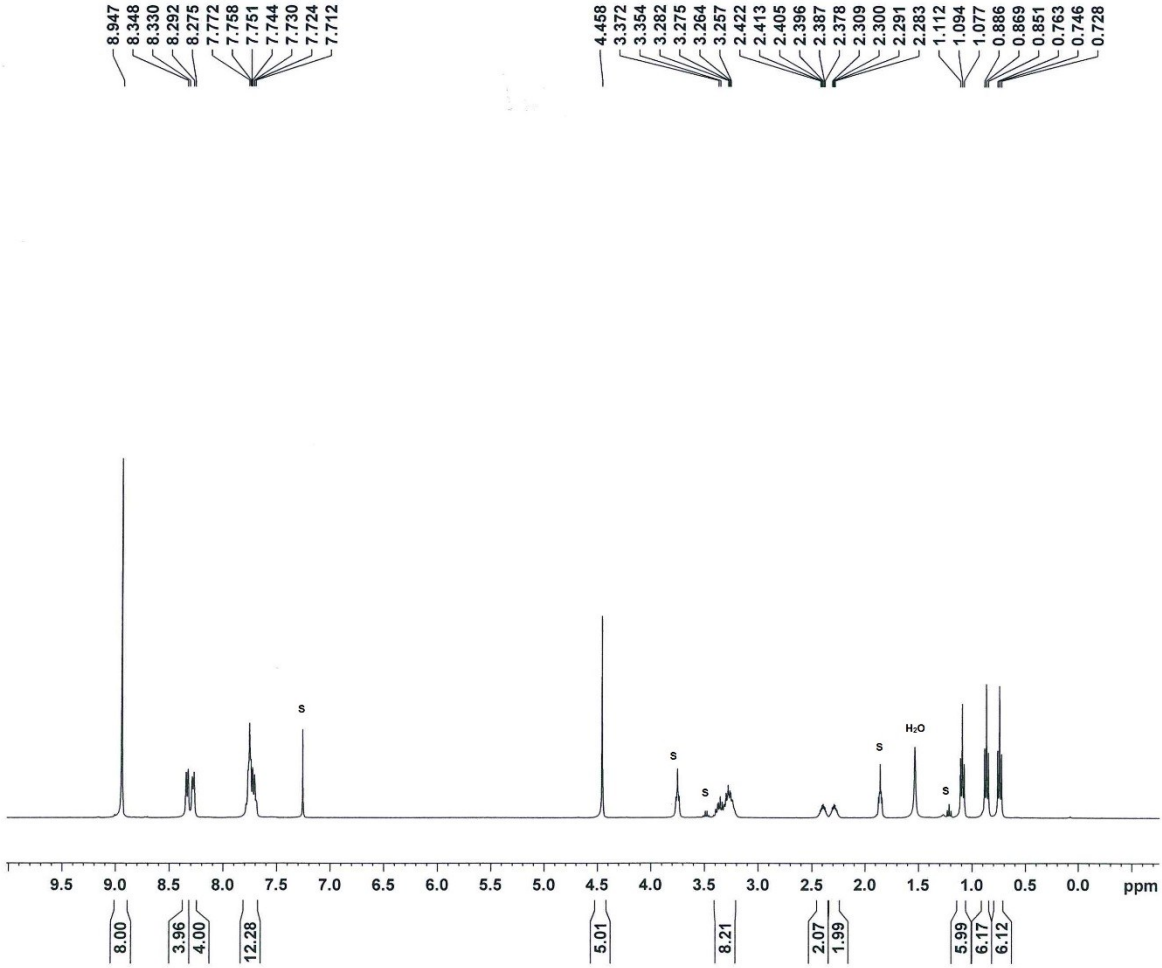


Figure S6. ^1H NMR (400 MHz, 298 K, CDCl_3) spectrum of **4** (X = impurity, S = residual solvent).

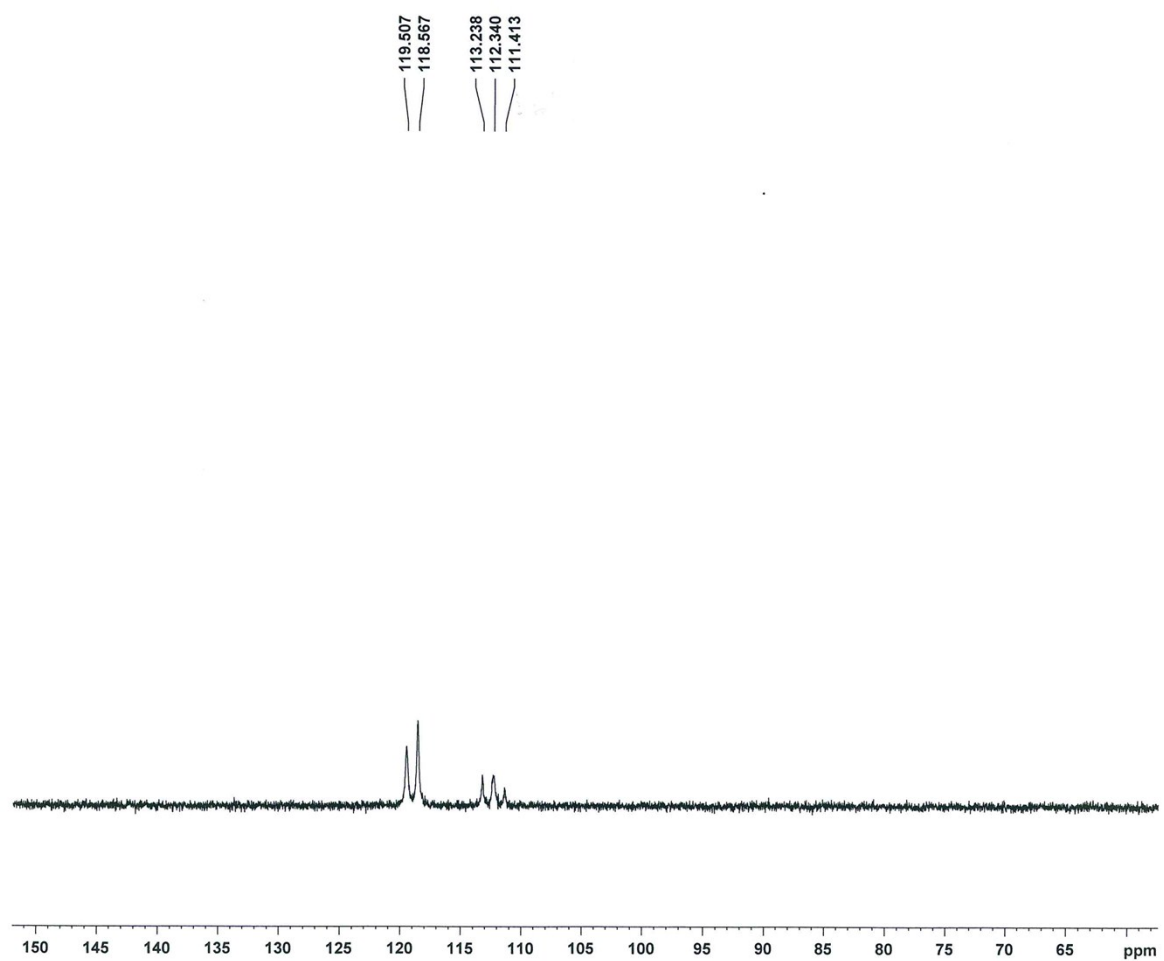


Figure S7. ¹H NMR (162 MHz, 298 K, CDCl₃) spectrum of **4**.

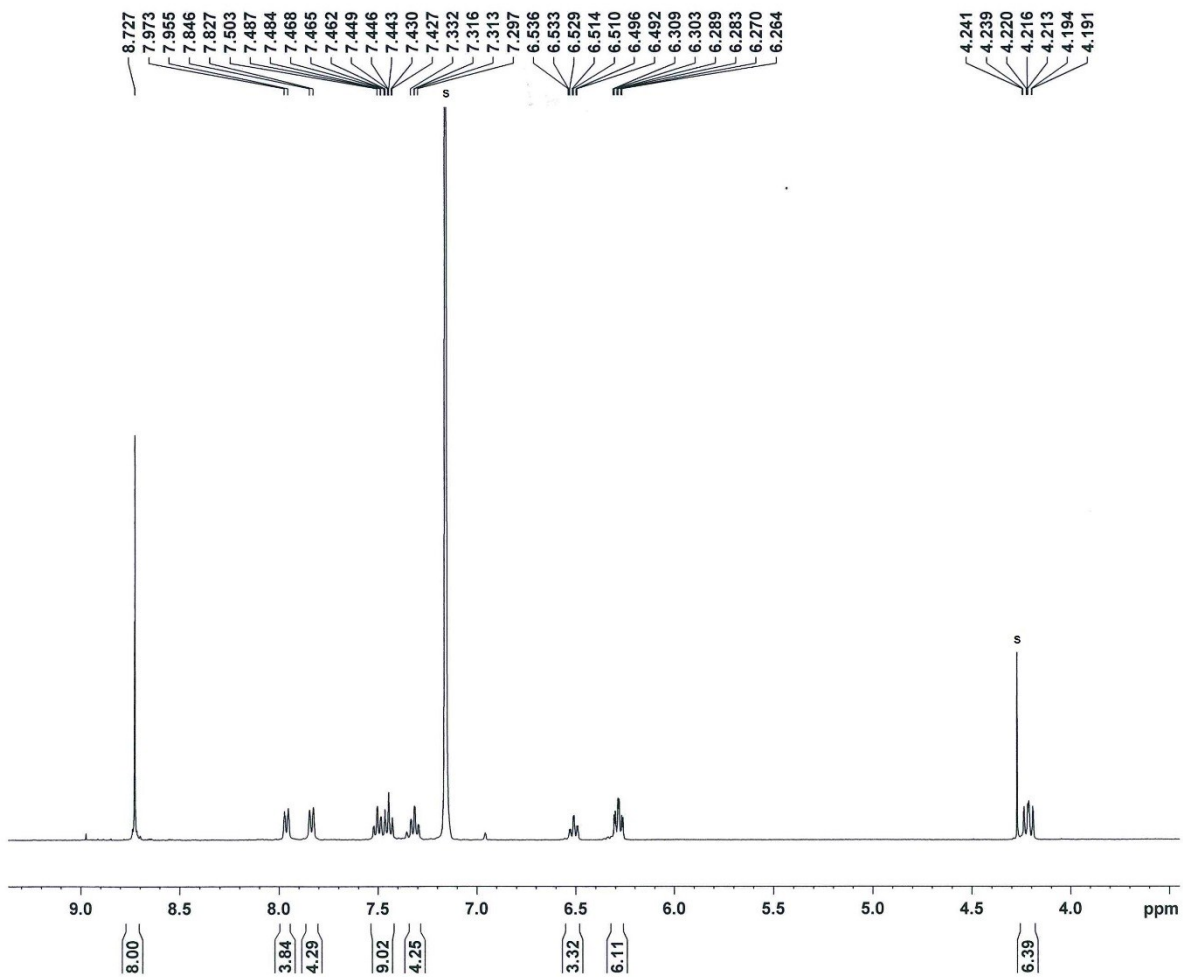


Figure S8. ^1H NMR (400 MHz, 298 K, C_6D_6) spectrum of **5** (X = impurity, S = residual solvent).

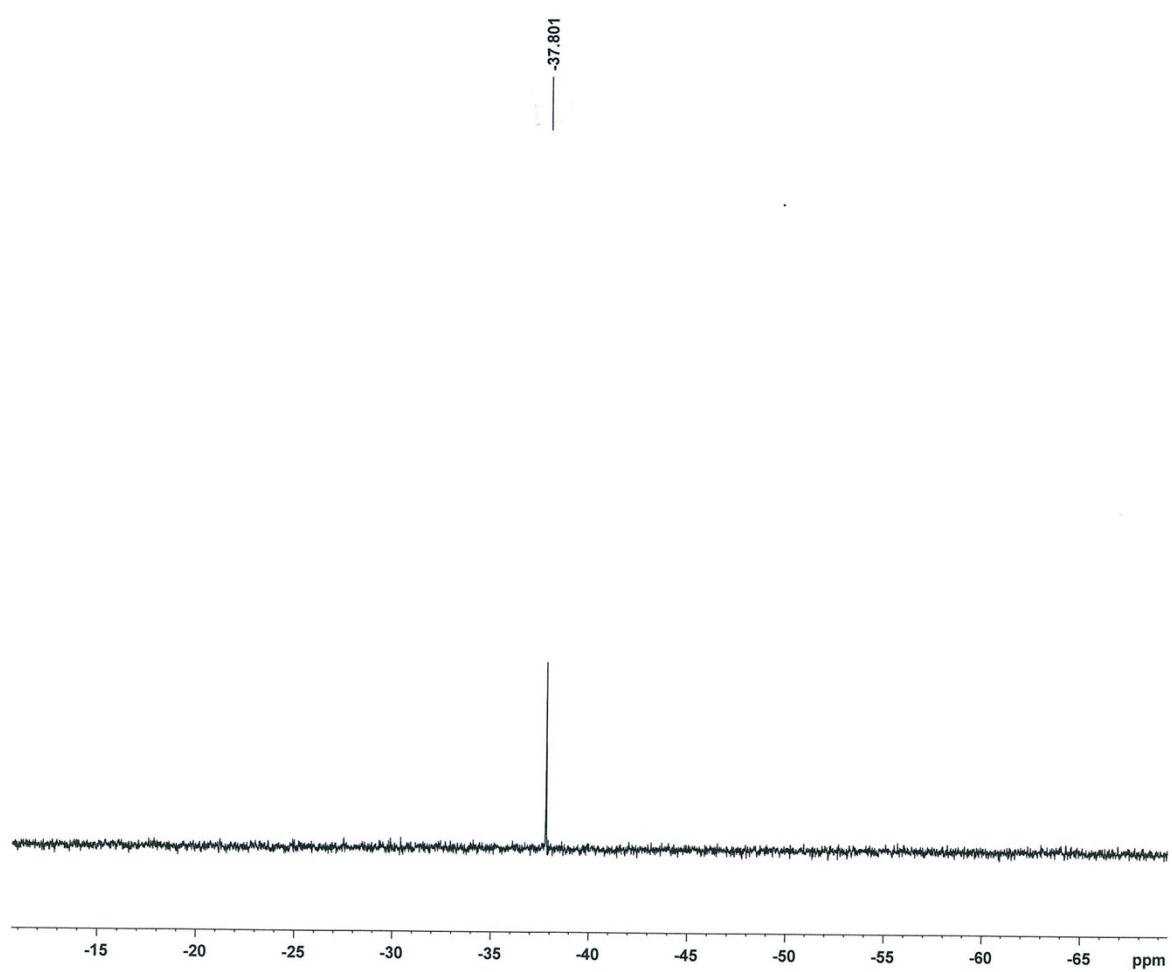


Figure S9. $^{31}\text{P}\{\text{H}\}$ NMR (162 MHz, 298 K, C_6D_6) spectrum of **5**.

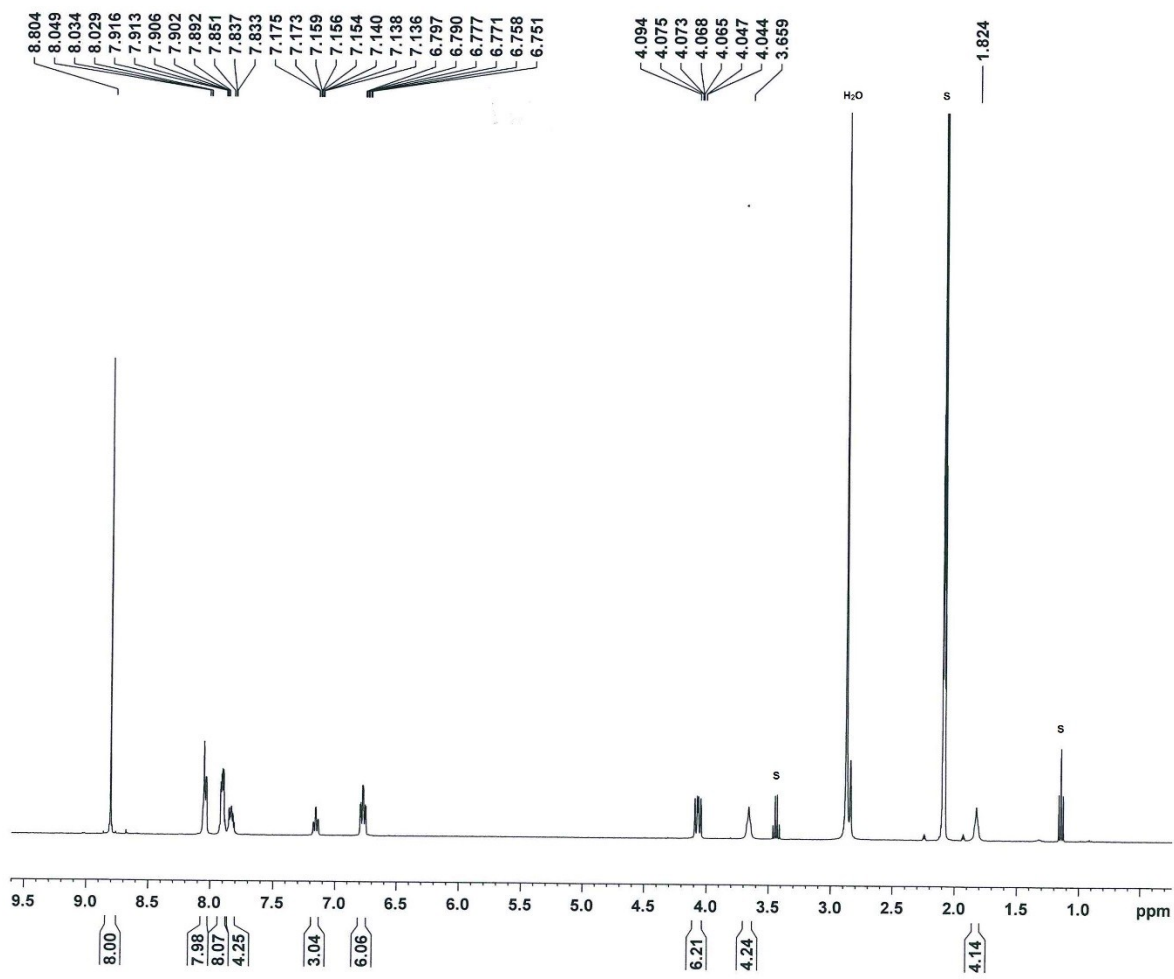


Figure S10. ^1H NMR (400 MHz, 298 K, acetone- d_6) spectrum of **6** (X = impurity, S = residual solvent).

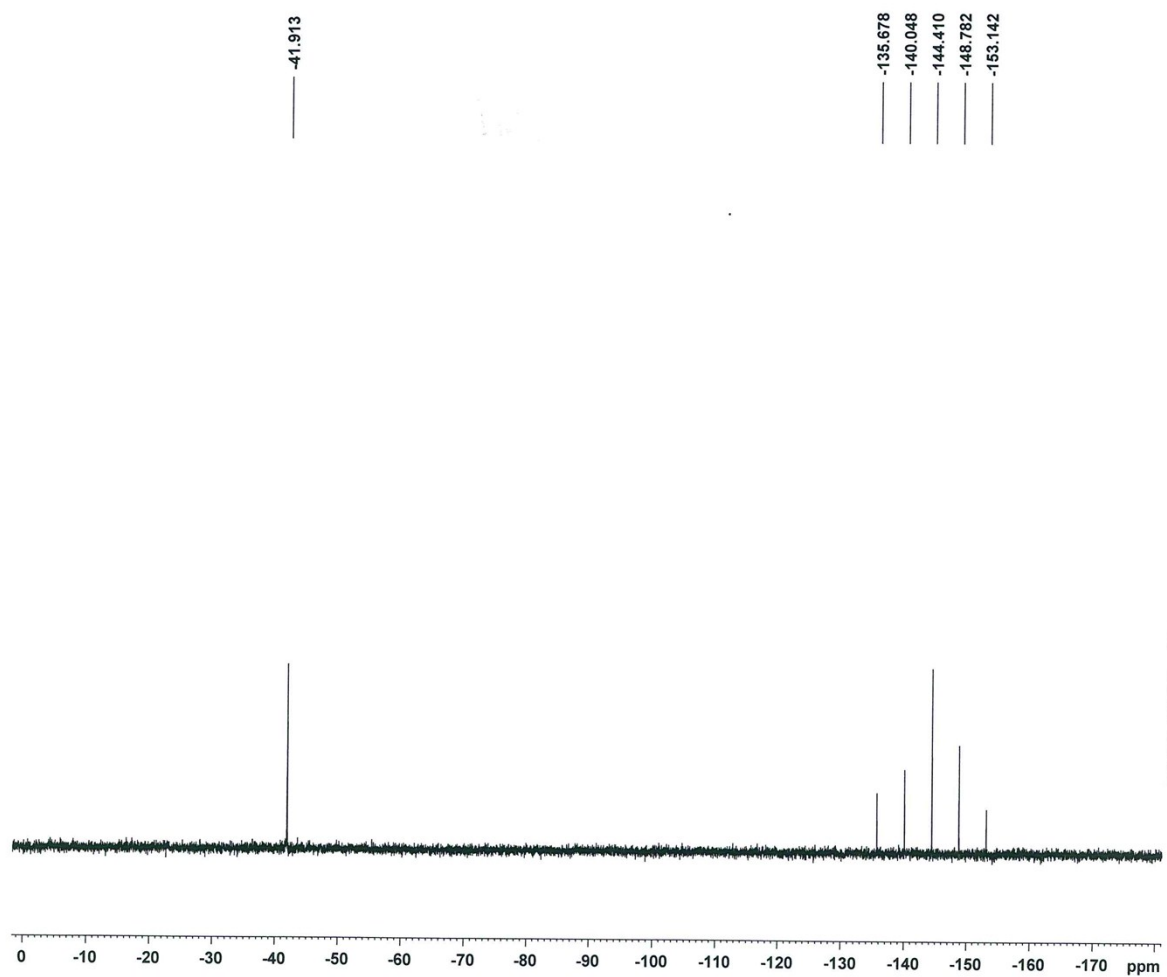


Figure S11. $^{31}\text{P}\{\text{H}\}$ NMR (162 MHz, 298 K, acetone- d_6) spectrum of **6**.

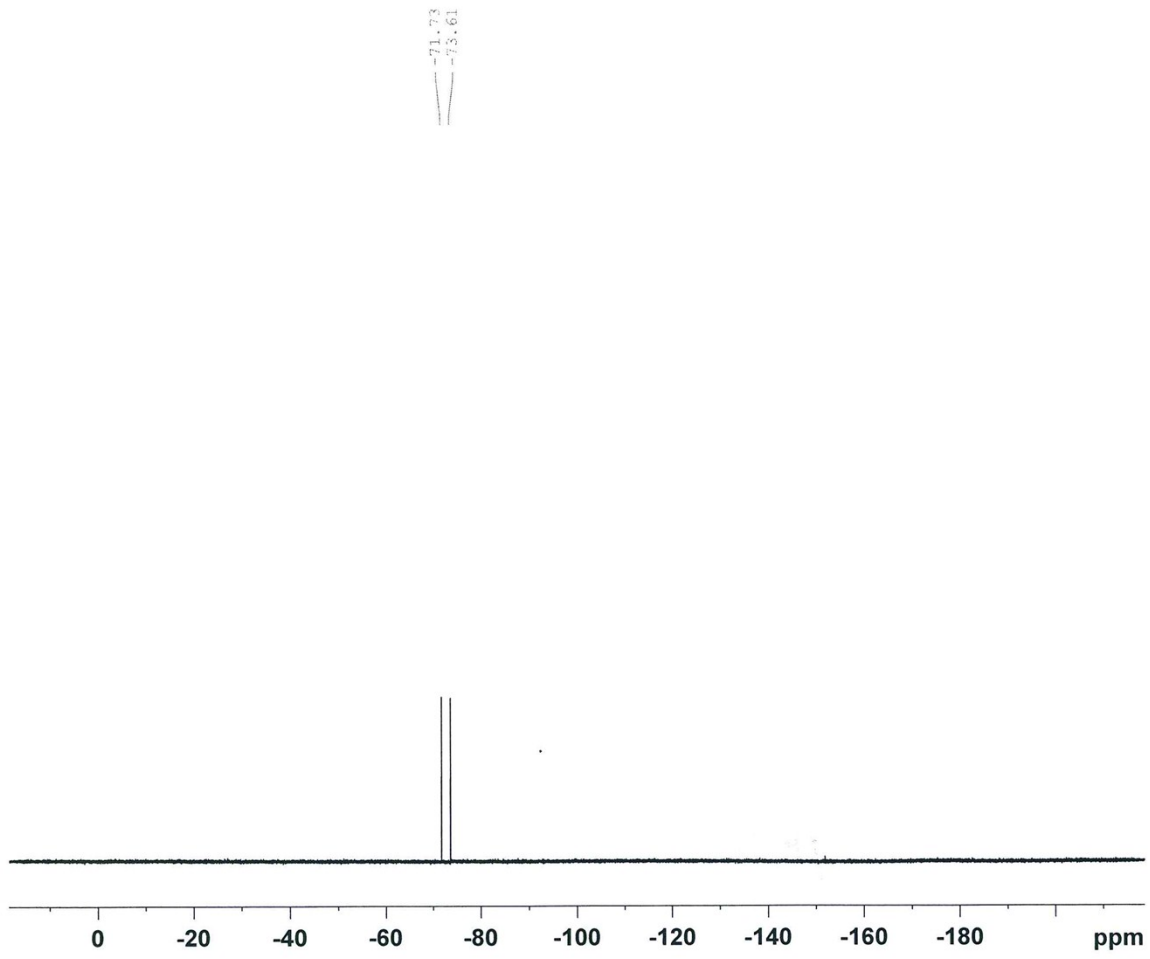


Figure S12. ${}^{19}\text{F}\{{}^1\text{H}\}$ NMR (376.5 MHz, 298 K, acetone- d_6) spectrum of **6**.

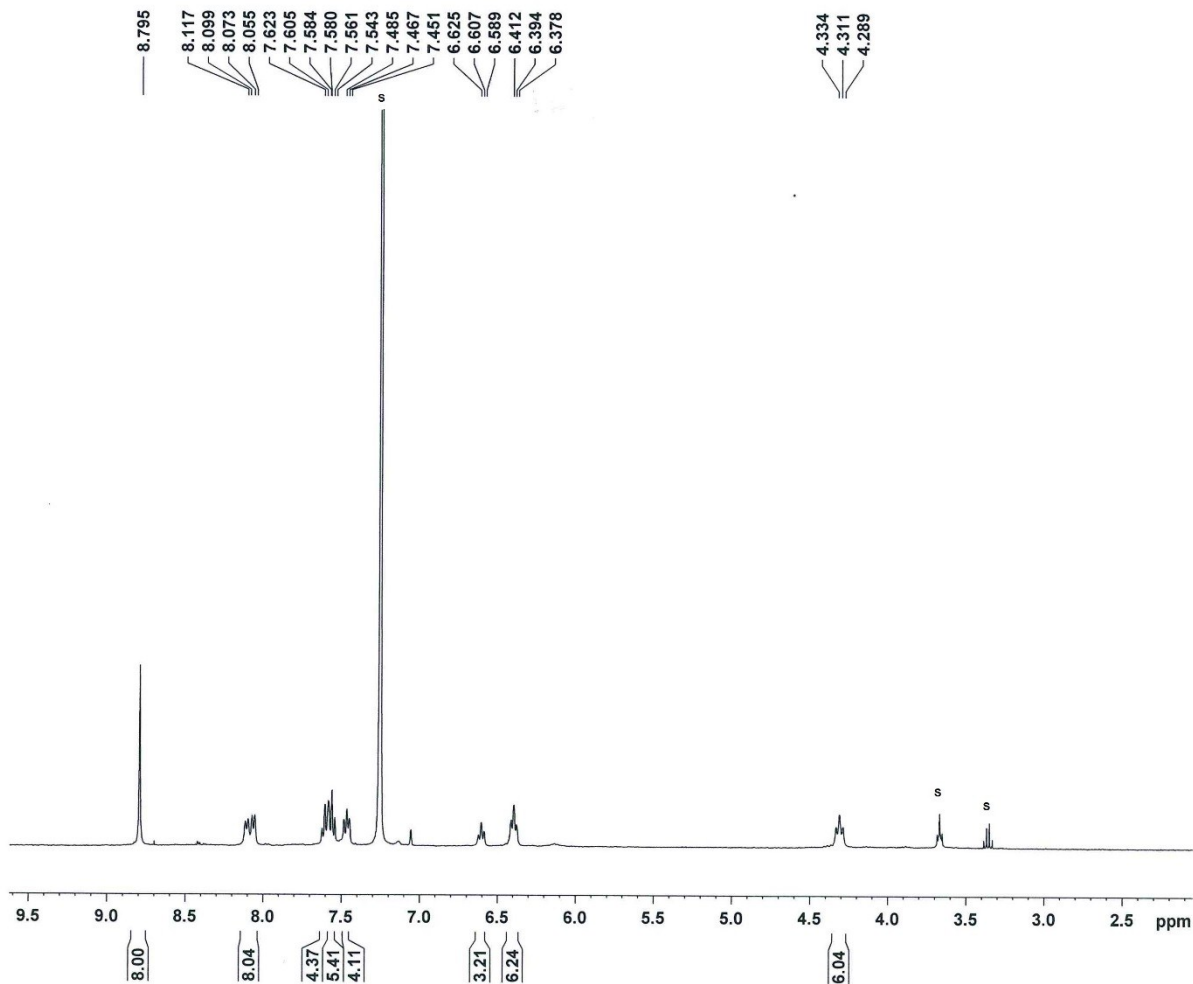


Figure S13. ^1H NMR (400 MHz, 298 K, C_6D_6) spectrum of **7** (X = impurity, S = residual solvent).

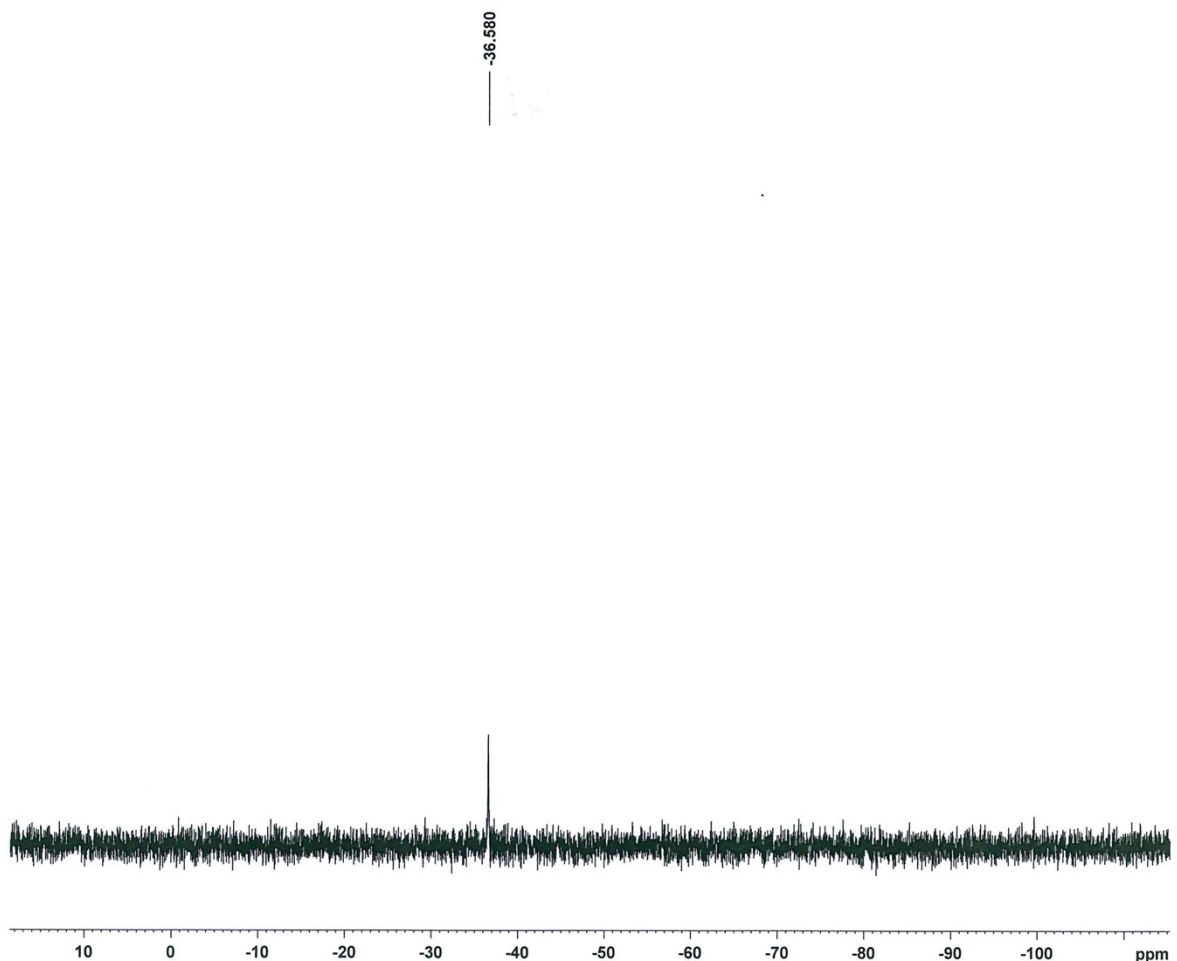


Figure S14. $^{31}\text{P}\{\text{H}\}$ NMR (162 MHz, 298 K, C_6D_6) spectrum of **7**.

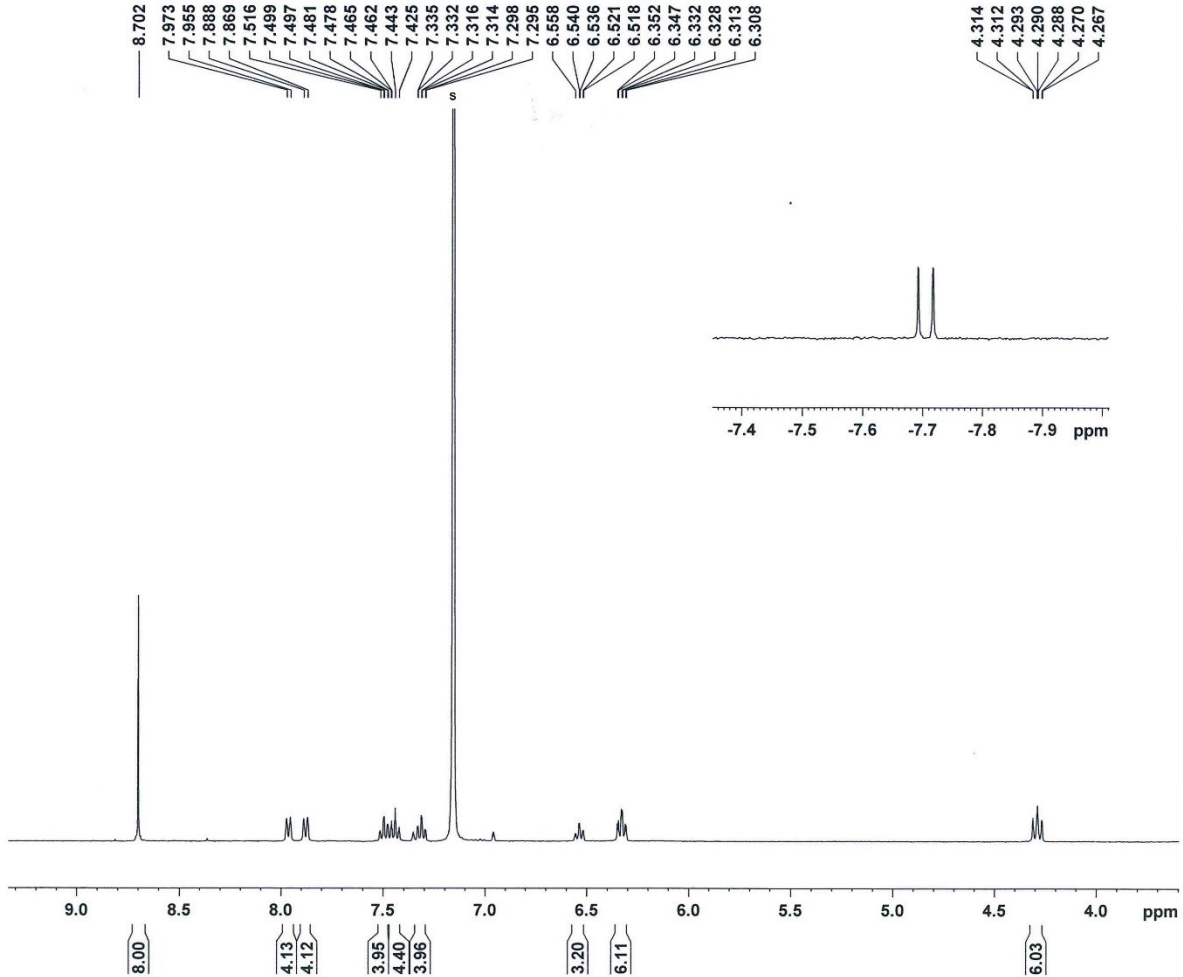


Figure S15. ^1H NMR (400 MHz, 298 K, C_6D_6) spectrum of **8** (X = impurity, S = residual solvent).

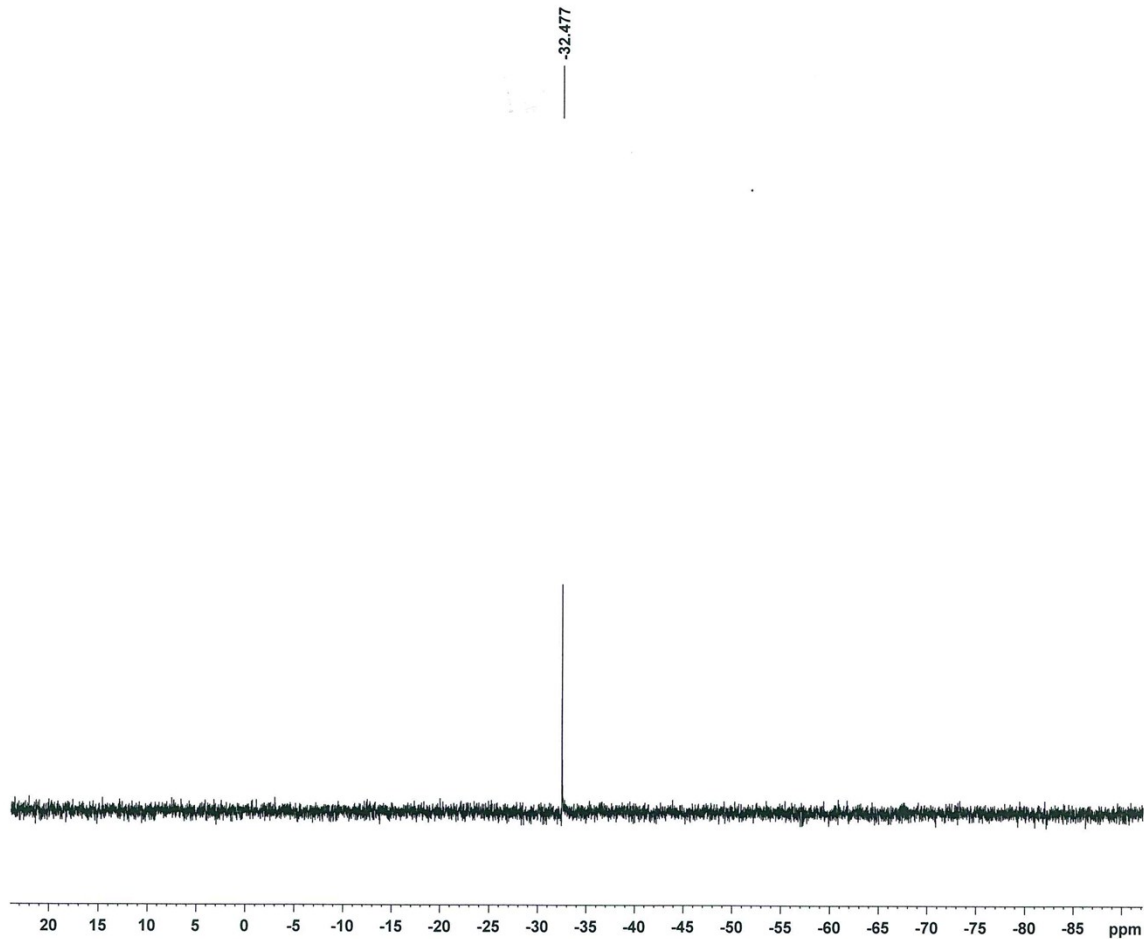


Figure S16. $^{31}\text{P}\{\text{H}\}$ NMR (162 MHz, 298 K, C_6D_6) spectrum of **8**.

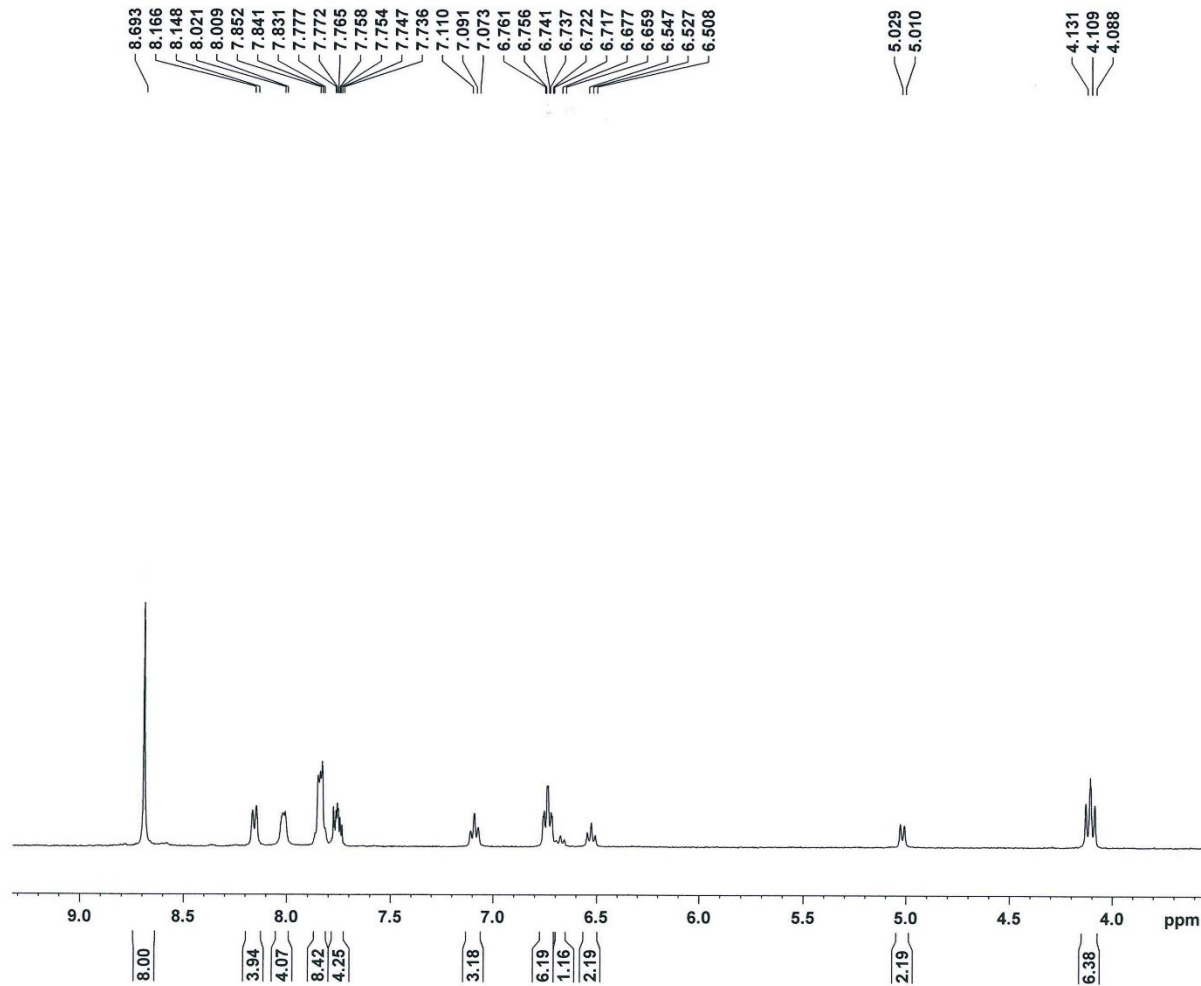


Figure S17. ^1H NMR (400 MHz, 298 K, acetone- d_6) spectrum of **9** (X = impurity, S = residual solvent).

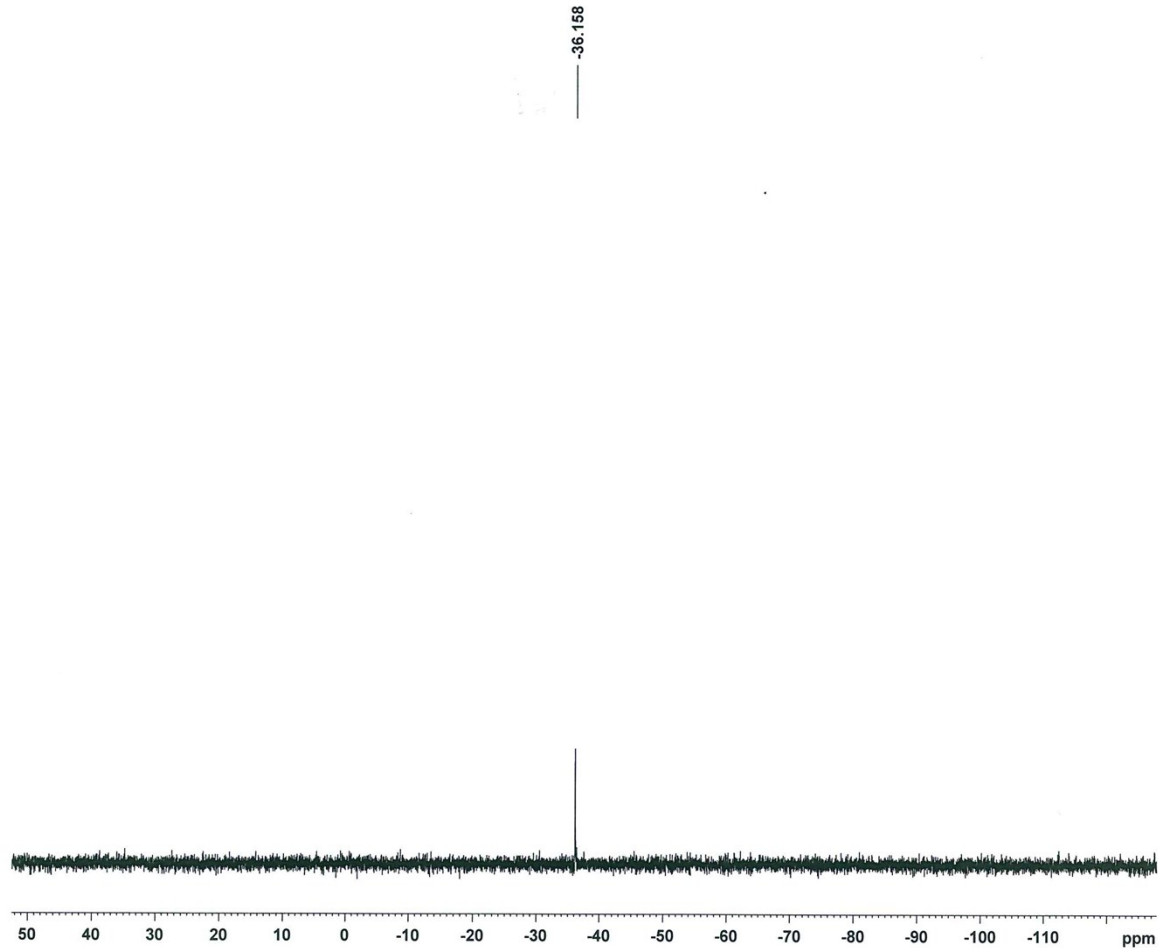


Figure S18. $^{31}\text{P}\{\text{H}\}$ NMR (162 MHz, 298 K, acetone- d_6) spectrum of **9**.

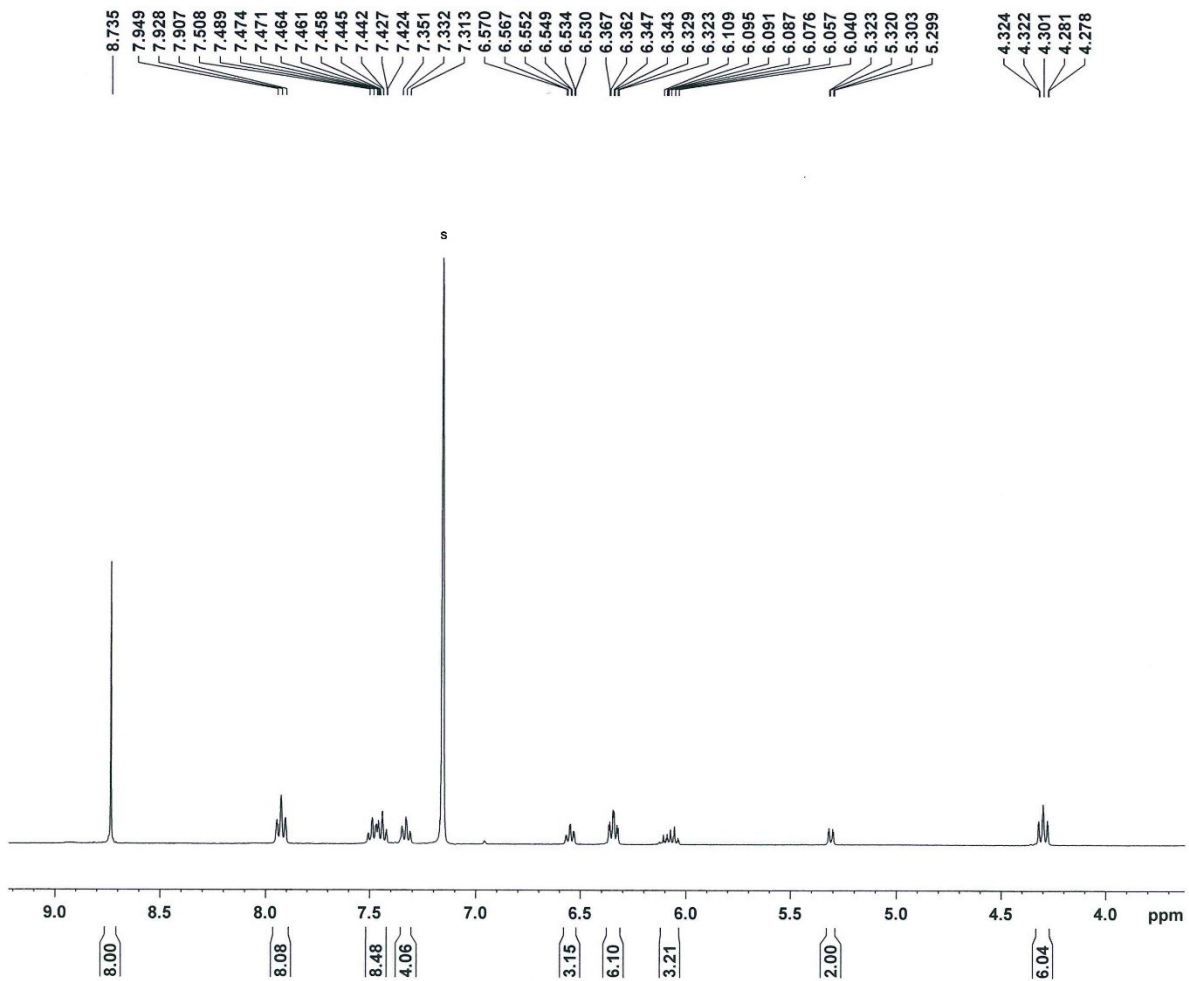


Figure S19. ${}^1\text{H}$ NMR (400 MHz, 298 K, C_6D_6) spectrum of **10** (X = impurity, S = residual solvent).

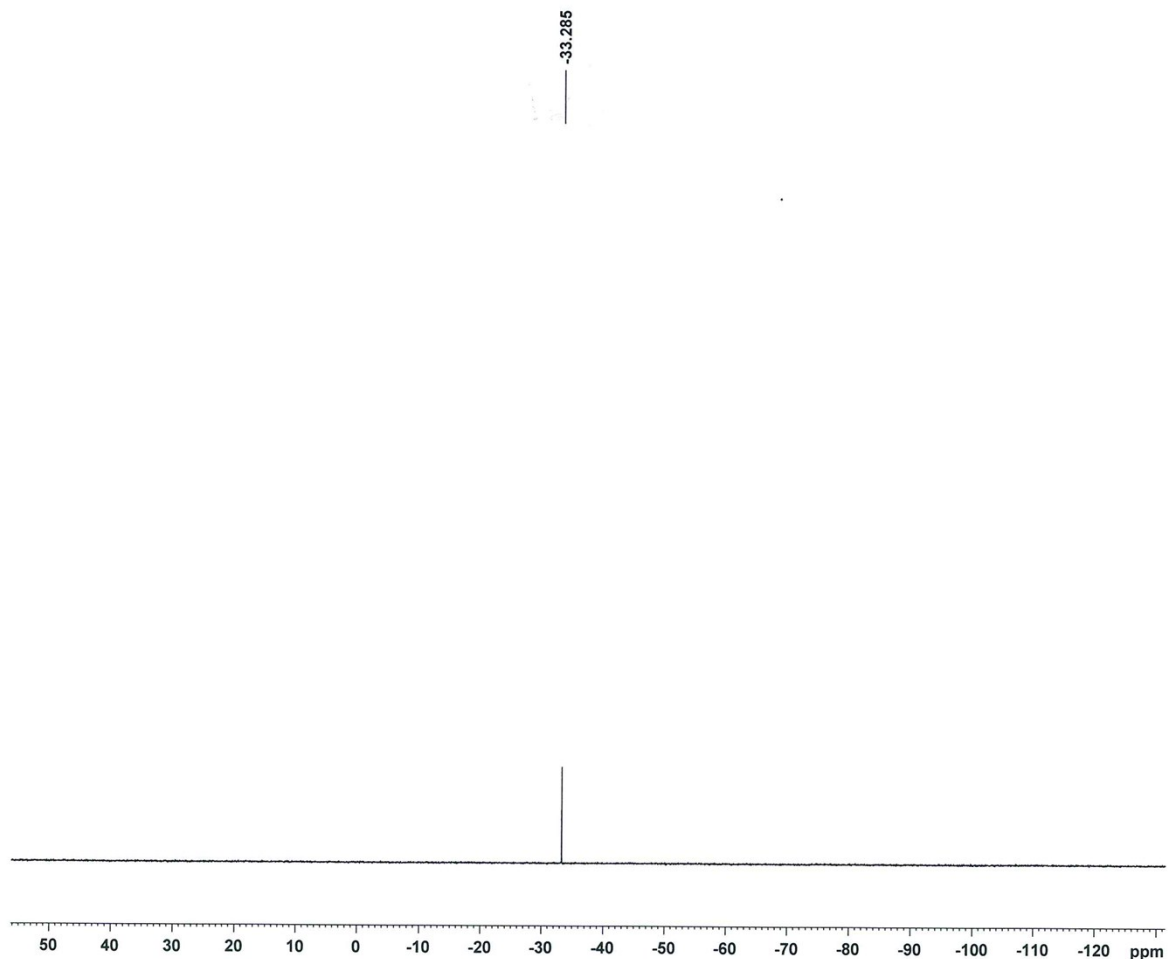


Figure S20. ${}^3\text{1}\text{P}\{{}^1\text{H}\}$ NMR (162 MHz, 298 K, C_6D_6) spectrum of **10**.

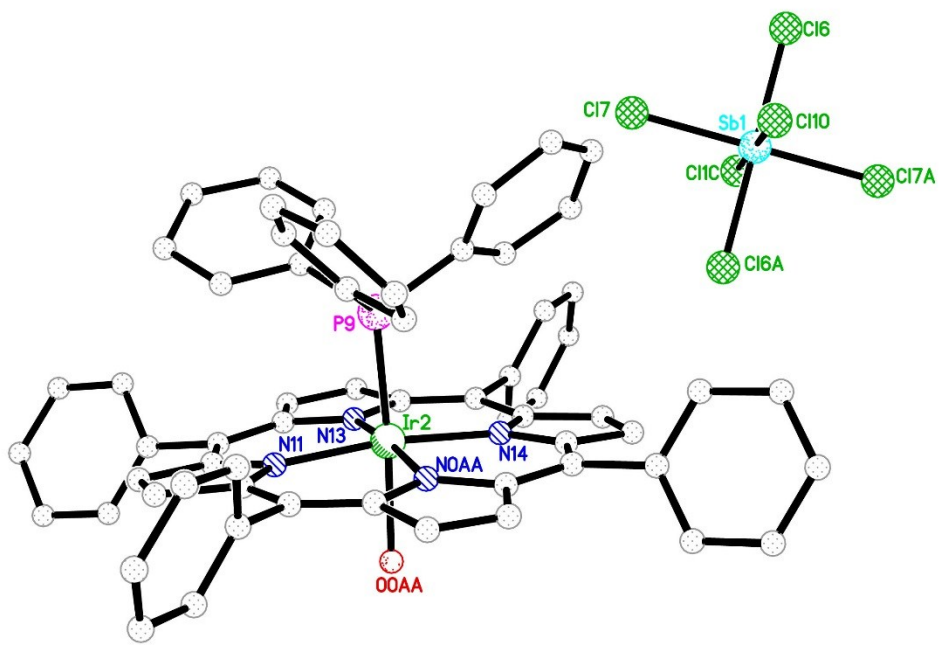


Figure S25. Preliminary molecular structure of $[\text{Ir}(\text{tpp})(\text{PPh}_3)(\text{H}_2\text{O})](\text{SbCl}_6)$.

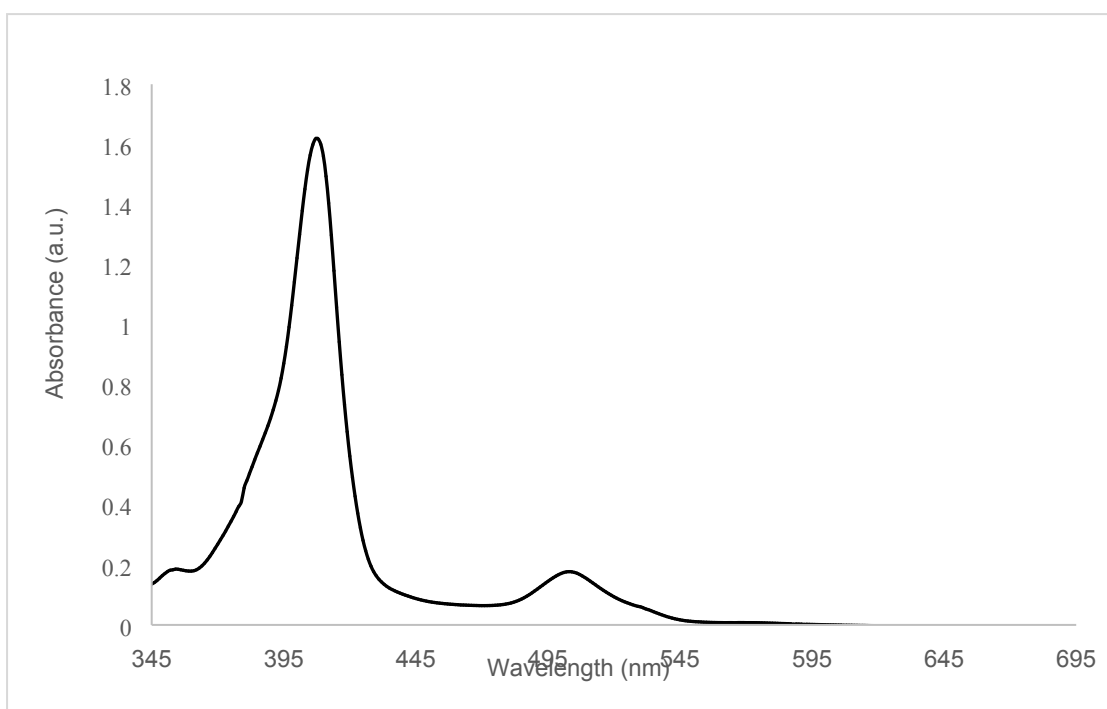


Figure S26. UV/vis spectrum of $[\text{Ir}(\text{tpp})\text{R}]$ ($\text{R} = \text{C}_8\text{H}_{13}$) (**1**) in CH_2Cl_2 at room temperature.

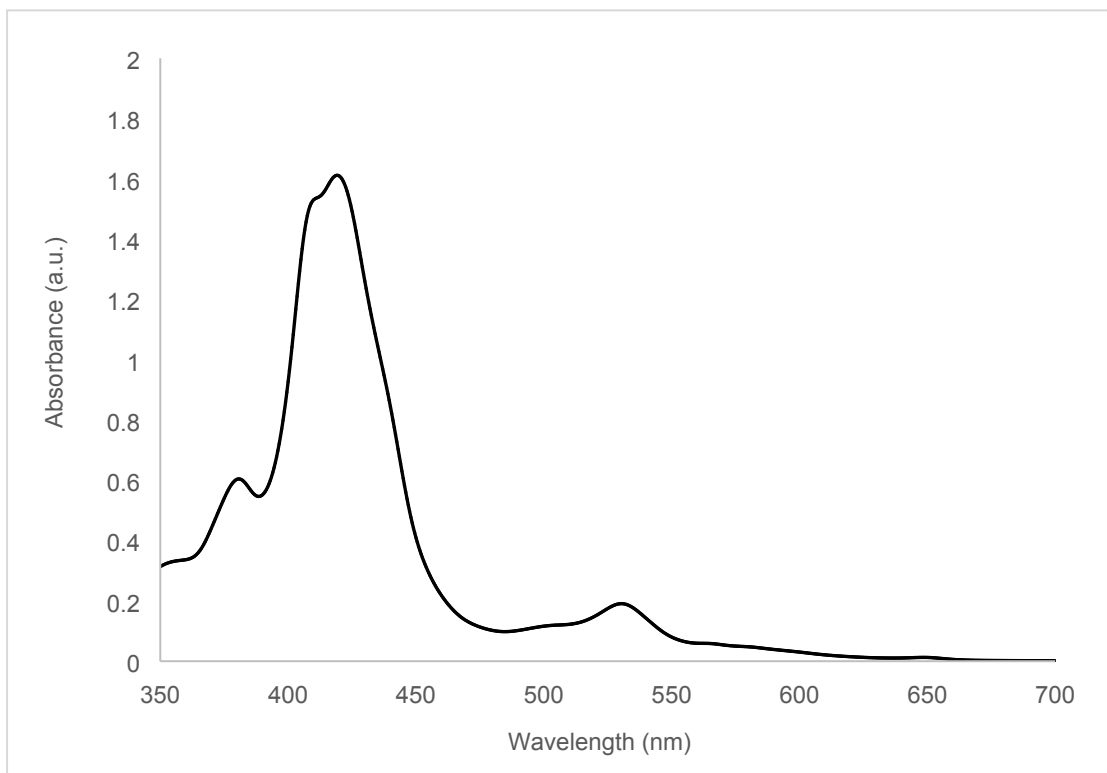


Figure S27. UV/vis spectrum of $[\text{Ir}(\text{tpp})(\text{C}_8\text{H}_{13})(\text{PPh}_3)]$ (**2**) in CH_2Cl_2 at room temperature.

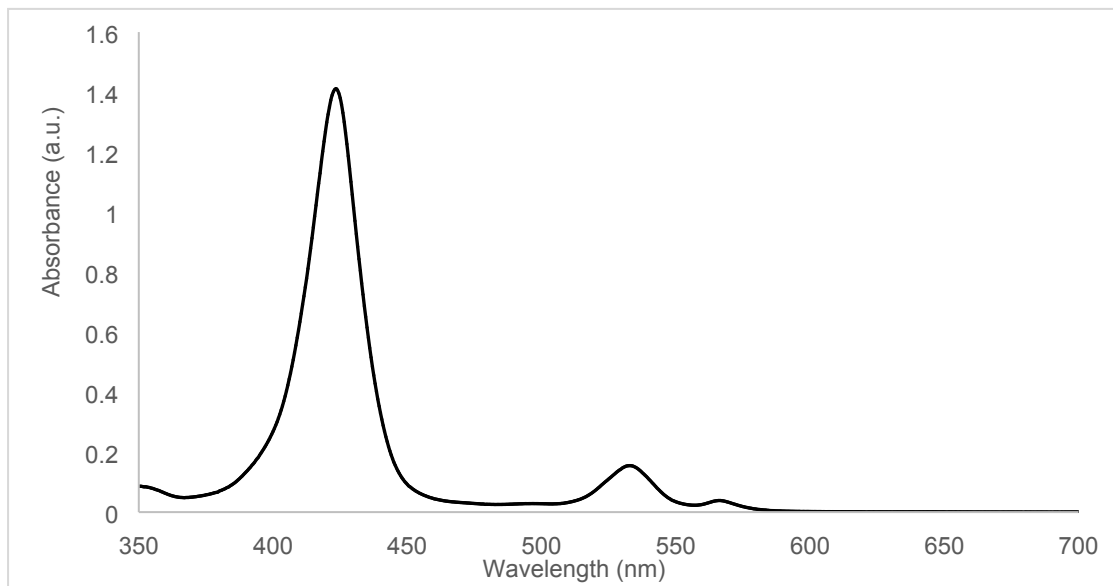


Figure S28. UV/vis spectrum of $[\text{Ir}(\text{tpp})(\text{PPh}_3)\text{Cl}]$ (**5**) in CH_2Cl_2 at room temperature.

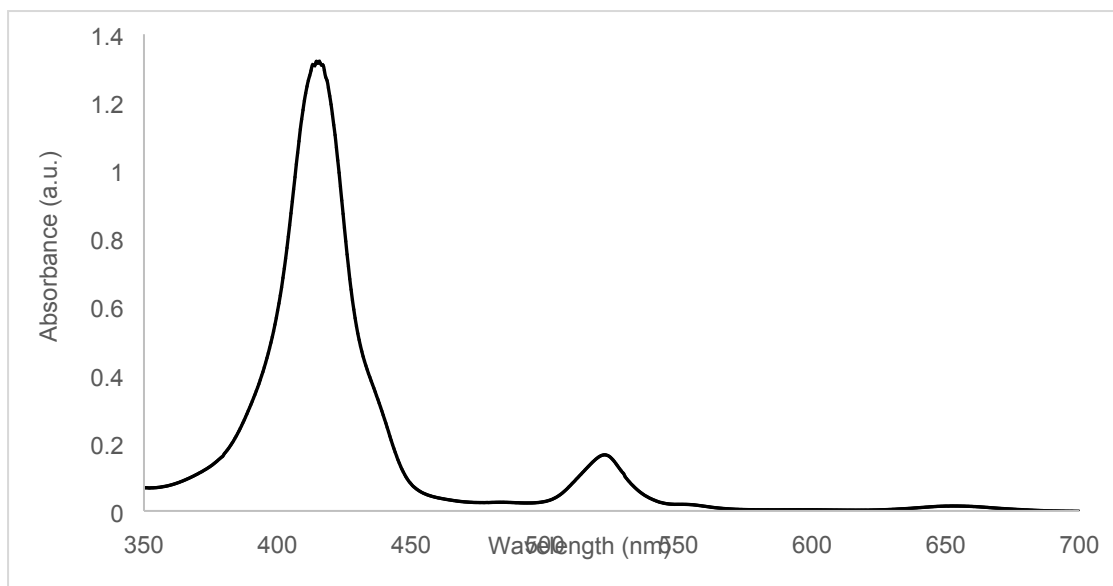


Figure S29. UV/vis spectrum of $[\text{Ir}(\text{tpp})(\text{PPh}_3)(\text{thf})](\text{PF}_6)$ (**6**) in CH_2Cl_2 at room temperature.

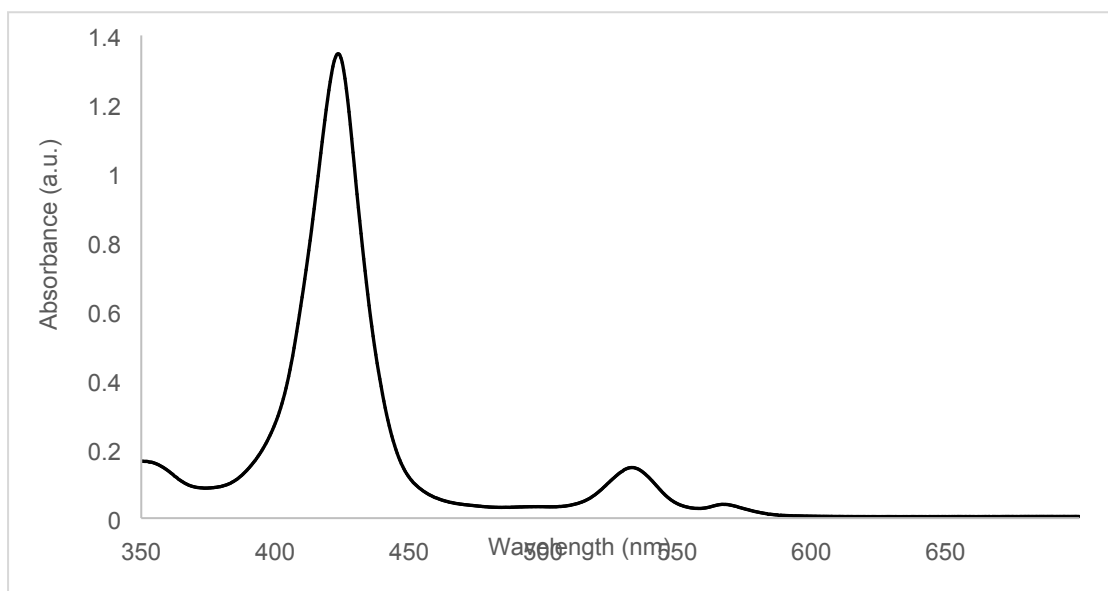


Figure S30. UV/Vis spectrum of $[\text{Ir}(\text{tpp})(\text{PPh}_3)(\text{OH})]$ (**7**) in CH_2Cl_2 at room temperature.

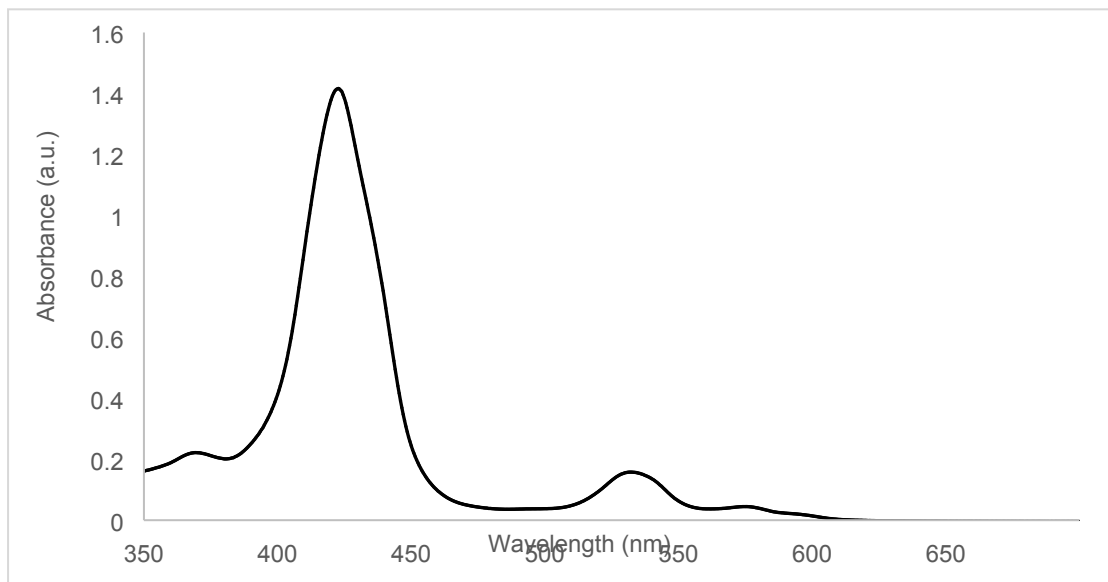


Figure S31. UV/Vis spectrum of $[\text{Ir}(\text{tpp})(\text{PPh}_3)(\text{SH})]$ (**8**) in CH_2Cl_2 at room temperature.

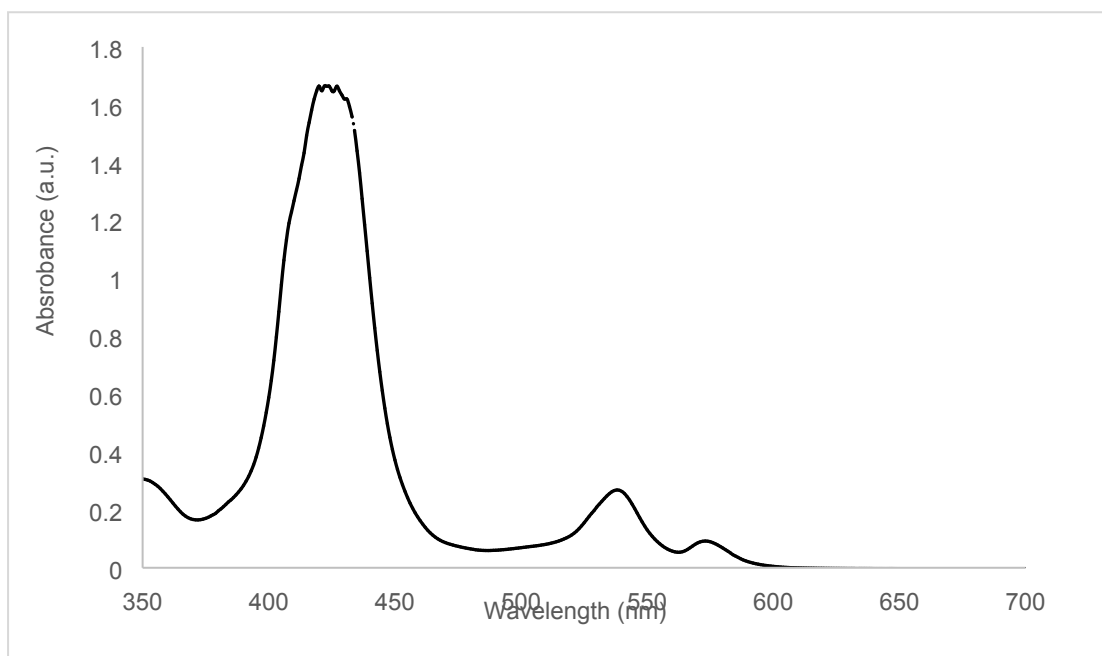


Figure S32. UV/Vis spectrum of $[\text{Ir}(\text{tpp})(\text{PPh}_3)(\mu\text{-}\eta^1\text{:}\eta^1\text{-C}\equiv\text{CPh})(\text{CuI})]$ (**9**) in CH_2Cl_2 at room temperature.

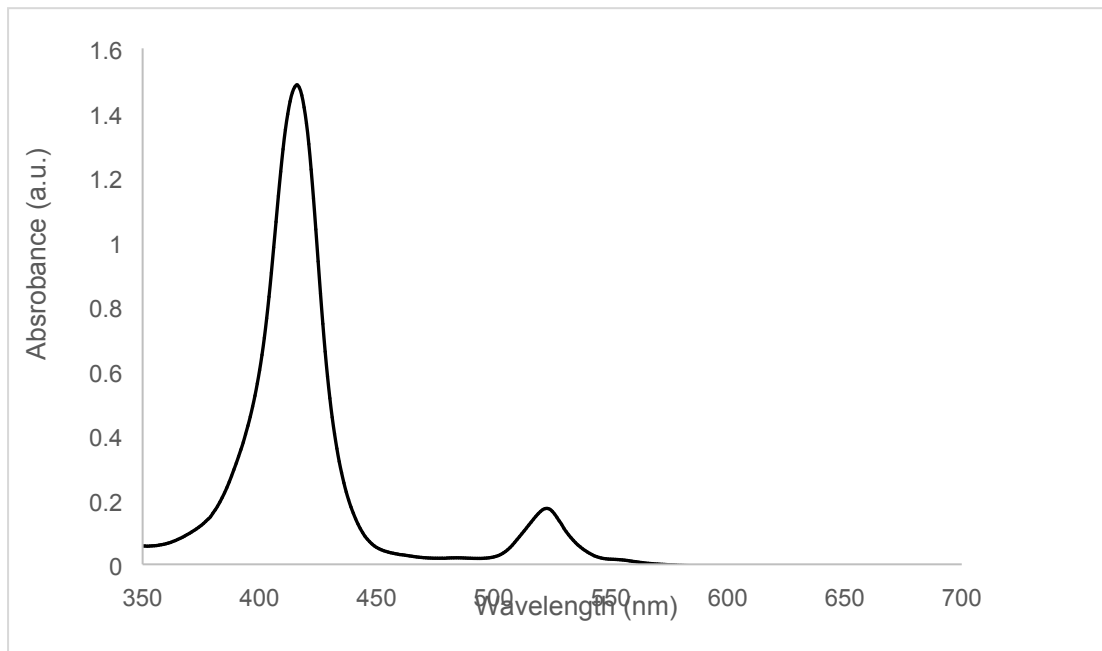


Figure S33. UV/Vis spectrum of $[\text{Ir}(\text{tpp})(\text{PPh}_3)(\text{C}\equiv\text{CPh})]$ (**10**) in CH_2Cl_2 at room temperature.

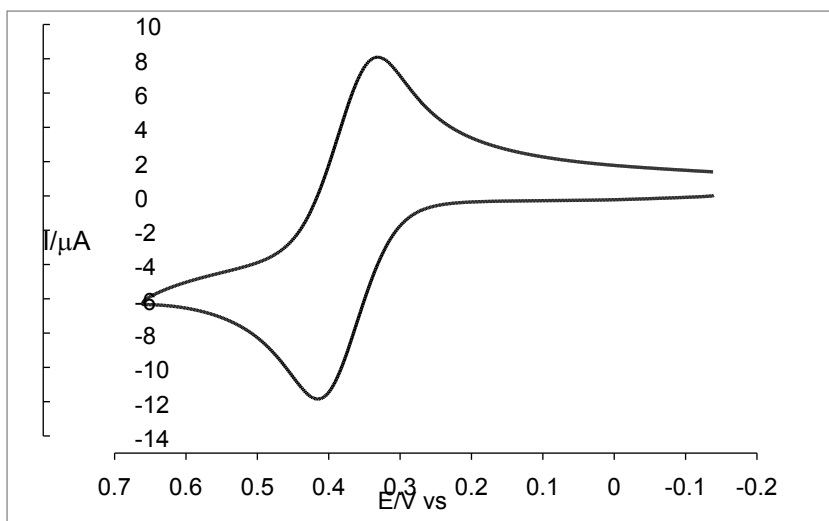


Figure S34. CV of $[\text{Ir}(\text{tpp})\text{R}]$ ($\text{R} = \text{C}_8\text{H}_{13}$) (**1**); measured at a glassy carbon electrode in CH_2Cl_2 , supporting electrolyte: 0.2 M of $[\text{nBu}_4\text{N}][\text{PF}_6]$, scan rate = 100 mVs^{-1} .

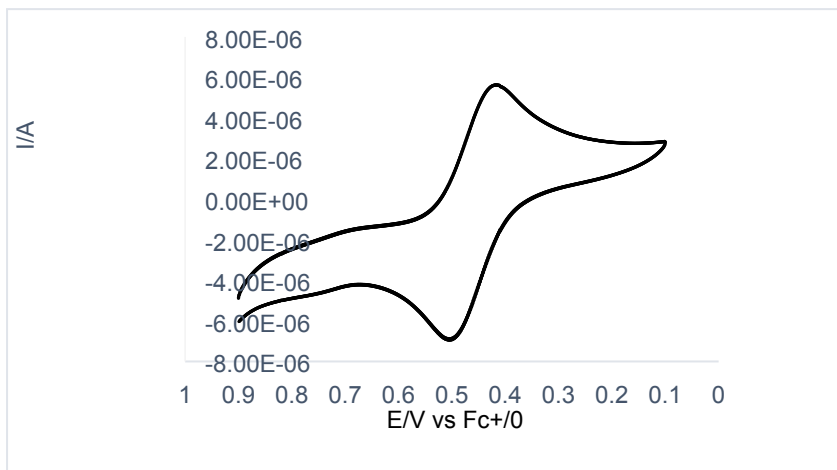


Figure S35. CV of $[\text{Ir}(\text{tpp})\text{R}(\text{PPh}_3)]$ ($\text{R} = \text{C}_8\text{H}_{13}$) (**2**); measured at a glassy carbon electrode in CH_2Cl_2 , supporting electrolyte: 0.2 M of $[\text{nBu}_4\text{N}][\text{PF}_6]$, scan rate = 100 mVs^{-1} .

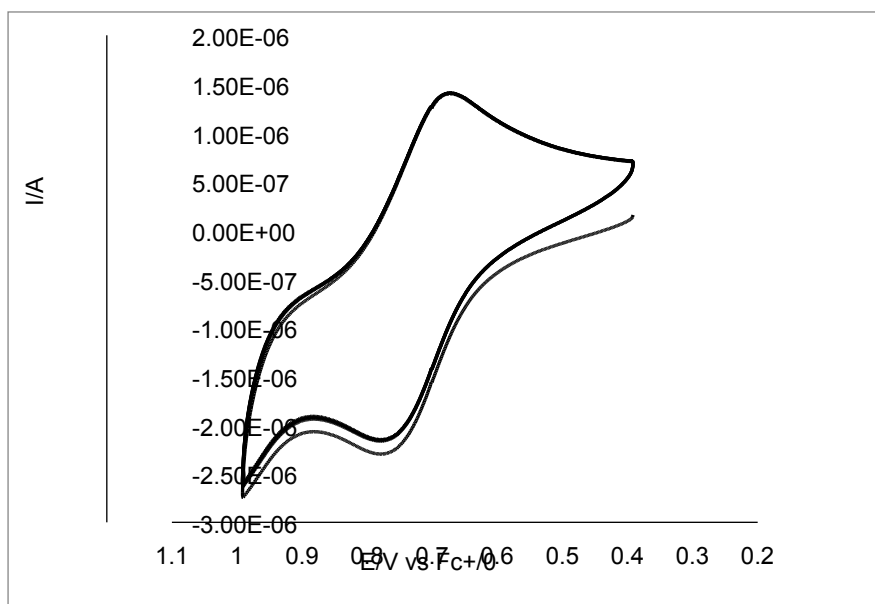


Figure S36. CV of $[\text{Ir}(\text{tpp})(\text{PPh}_3)\text{Cl}]$ (**5**); measured at a glassy carbon electrode in CH_2Cl_2 , supporting electrolyte: 0.2 M of $[^n\text{Bu}_4\text{N}][\text{PF}_6]$, scan rate = 100 mVs^{-1} .

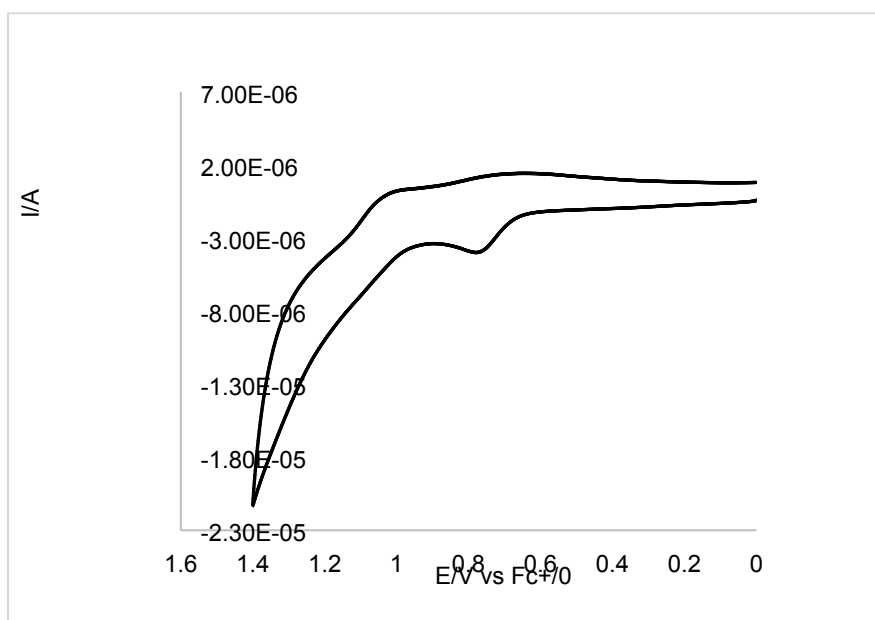


Figure S37. CV of $[\text{Ir}(\text{tpp})(\text{PPh}_3)(\text{OH})]$ (**7**); measured at a glassy carbon electrode in CH_2Cl_2 , supporting electrolyte: 0.2 M of $[^n\text{Bu}_4\text{N}][\text{PF}_6]$, scan rate = 100 mVs^{-1} .

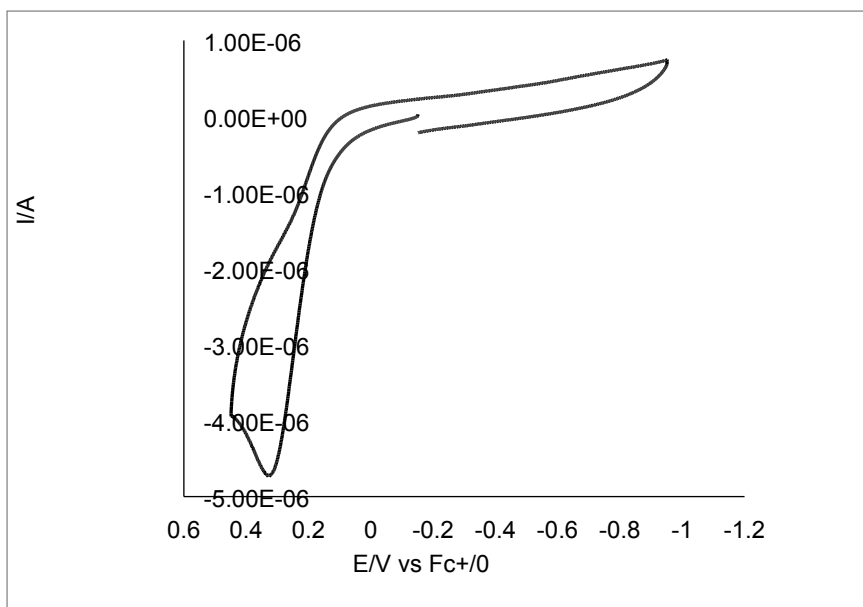


Figure S38. CV of $[\text{Ir}(\text{tpp})(\text{PPh}_3)(\text{SH})]$ (**8**); measured at a glassy carbon electrode in CH_2Cl_2 , supporting electrolyte: 0.2 M of $[^n\text{Bu}_4\text{N}][\text{PF}_6]$, scan rate = 100 mVs⁻¹.

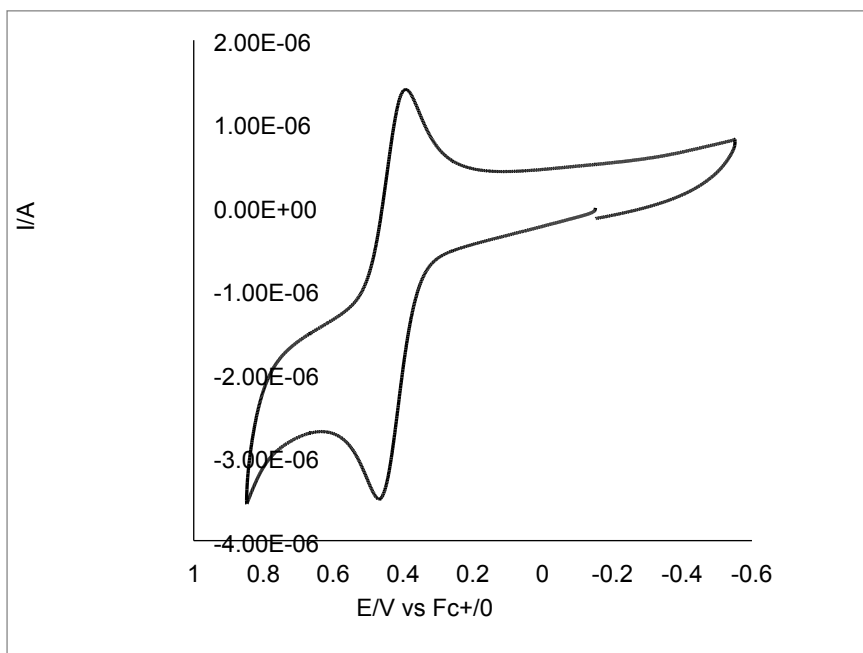


Figure S39. CV of $[\text{Ir}(\text{tpp})(\text{PPh}_3)(\text{C}\equiv\text{CPh})]$ (**10**); measured at a glassy carbon electrode in CH_2Cl_2 , supporting electrolyte: 0.2 M of $[^n\text{Bu}_4\text{N}][\text{PF}_6]$, scan rate = 100 mVs⁻¹.